Electronic Supplementary Material (ESI) for RSC Advances.

Table s1. Spectroscopic data for all compounds.

Compound	IR; ν(CO) cm^{-1}	^{1}H NMR; δ(SCH) ppm	^{13}C NMR; δ(CO) ppm
Y1	1515	4.20	182.50
1	1646	4.93 (trans) 5.62 (cis)	194.48
Y2	1539	4.35	178.05
2	1630	5.05 (trans) 5.66 (cis)	192.17
Y3	1537	4.20	180.09
3	1637	5.10 (trans) 5.71 (cis)	193.87

Table s2. Selected bond lengths [Å] and angles [°] for structure of **3**.

Bond Lengths	**Value**
Pd(1)-Cl(1)	2.3449(9)
Pd(1)- Cl(1)1	2.3449(9)
Pd(1)- C(1)	2.118(5)
Pd(1)- Cl(1)1	2.118(5)
S(1)-C(1)1	1.787(5)
S(1)-C(1)	1.781(6)
S(1)-C(9)	1.815(5)
O(1)- C(10)	1.233(6)
O(2)- C(2)	1.207(6)
O(3)- N(1)	1.218(6)
Bond angles	**Value**
Cl(1)-Pd(1)-Cl(1)1	180.0
C(1)1-Pd(1)-Cl(1)1	91.68(13)
C(1)-Pd(1)-Cl(1)	91.68(13)
C(1)-Pd(1)-Cl(1)1	88.32(13)
C(1)1-Pd(1)-Cl(1)	88.32(13)
C(1)1-Pd(1)-C(1)	180.0
C(1)-S(1)-C(10)	104.4(2)
C(9)-S(1)-C(1)	102.7(3)
C(9)-S(1)-C(10)	100.2(3)
O(2)-N(1)-O(3)	123.4(5)
O(2)-N(1)-C(6)	118.8(4)
O(3)-N(1)-C(6)	117.9(4)
S(1)-C(1)-Pd(1)	107.8(2)
C(2)-C(1)-Pd(1)	112.3(3)

Table s3. Selected bond lengths [A°] and bond angles [°] of complexes 1-3 at the BP86/def2-SVP level of theory.

1		**2**		**3**	
Bond distance	Value	Bond distance	Value	Bond distance	Value
Pd1-C5	2.12	Pd1-C5	2.13	Pd1-C8	2.129(2.118)[a]
Pd1-C28	2.12	Pd1-C28	2.13	Pd1-C35	2.129(2.118)
Pd1-Cl2	2.36	Pd1-Cl2	2.35	Pd1-Cl29	2.354(2.345)
Pd1-Cl25	2.36	Pd1-Cl25	2.35	Pd1-Cl2	2.354(2.345)
Bond angles	Value	Bond angles	Value	Bond angles	Value
C5-Pd1-C28	180.0	C5-Pd1-C28	180.0	C8-Pd1-C35	180.0(180.0)
Cl2-Pd1-Cl25	180.0	Cl2-Pd1-Cl25	180.0	Cl2-Pd1-Cl29	180.0(180.0)
C5-Pd1-Cl2	92.29	C5-Pd1-Cl2	92.48	C8-Pd1-Cl2	92.70(91.68)
C5-Pd1-Cl25	87.70	C5-Pd1-Cl25	87.52	C35-Pd1-Cl2	87.30(88.32)
Cl28-Pd1-Cl25	92.30	Cl28-Pd1-Cl25	92.48	C35-Pd1-Cl29	92.70(91.68)
C28-Pd1-Cl2	87.71	C28-Pd1-Cl2	87.52	C8-Pd1-Cl29	87.30(88.32)

[a] The experimental values are given in parenthesis.

Table s4. The most important donor→ acceptor interactions energy concern to Pd–C bonds at BP86/def2-SVP level of theory

Donor	Acceptor	Type	E^2 (kcal/mol)
Complex 1			
Pd (1) – C(28)	Pd (1) –Cl(25)	$\sigma \rightarrow \sigma^*$	15.45
Pd (1) – C(28)	S(26) – C(44)	$\sigma \rightarrow \sigma^*$	4.57
Complex 2			
Pd (1) – Cl(2)	Pd (1) – Cl(2)	$\sigma \rightarrow \sigma^*$	5.31
Pd (1) – C(28)	Pd (1) – C(28)	$\sigma \rightarrow \sigma^*$	20.55
Pd (1) – C(28)	Pd (1) – C(28)	$\sigma \rightarrow \sigma^*$	15.01
Pd (1) – C(28)	S(26) – C (44)	$\sigma \rightarrow \sigma^*$	4.50
Complex 3			
Pd (1) – Cl(29)	Pd (1) – Cl(29)	$\sigma \rightarrow \sigma^*$	5.19
Pd (1) – Cl(29)	Pd (1) – Cl(29)	$\sigma \rightarrow \sigma^*$	19.69
Pd (1) – C(35)	Pd (1) – Cl(29)	$\sigma \rightarrow \sigma^*$	15.42
Pd (1) – C(35)	O(31) – C (37)	$\sigma \rightarrow \sigma^*$	14.07

Optimization of Mizoroki-Heck reaction.

In the first optimization, we explore the effect of the catalyst loading on the reaction. Catalyst concentration has an important effect on the reaction proceed. If the concentration of complex **3** decreased, the yield of reaction shows a beat decrease (Table 9, entry 2). At the very low catalyst concentration (0.001 mmol), the performance of catalyst falls down and will be stop as if the catalyst was not there (Table 9, entries 3 and 4). Also, excessive amount of catalyst did not increase the yields significantly (Table 9, entry 5). Therefore, the low catalyst concentration of 0.005 mmol was chosen as the best economically catalyst loading.

Having the 0.005 mmol of catalyst, the solvent optimization stage was done with several commonly used solvents. Polar aprotic solvents such as DMF, NMP and EtOH gave excellent conversions at reflux temperature (Table 9, Entries 1, 6 and 7, respectively). However, water required additional time for completing coupling reaction (Table 9, Entry 8). Also, non-polar solvents such as toluene and hexane were tested and results showed that the conversion for the desired coupling product was low (Table 9 Entries 9 and 10).

Next, we test some of organic and inorganic bases such as amines and carbonates to explore the effect of base. It has usually plays important roles in such cross-coupling reactions which can accelerate reaction proceed. Among the tested inorganic bases, Cs_2CO_3 has the most accelerating effect (Table 9, entry 12), while other bases, K_2CO_3, Na_2CO_3, and NaOAc proved to be less active (Table 9, Entries 2, 11 and 13). Organic base NEt_3 or pyridine shows inferior results and slow reaction rates compared to inorganic bases (Table 9, entries 14 and 15).

Finally, the reactions were carried out at different temperature. As the temperature of the reactions was decreased, increasing the reaction time for completion was observed (Table 9, entries 16-18). So, the reactions were performed at reflux temperature to gives the coupled products at highest yield.

In order to choosing the best catalyst from the complexes **1-3**, the catalytic activities of these complexes were studied in same reaction conditions (Table 9, entries 19 and 20). The catalytic activity showed that complex **3** (87%) was superior to the other **1** and **2** (76 and 82%) complexes. Although these catalytic performances are not so distinguishable, it seems that the catalytic activity of the Pd(II) complexes depending on the position of the phenyl ring substituent, and increasing in this order: 4-nitrophenyl (**3**)> 3-nitrophenyl (**2**)> phenyl (**1**). This trend seems to fit the electronic nature and position of the substituents on phenyl ring, in which the electron-withdrawing $-NO_2$ group at the *para* position has more capability to stabilize sulfur ylide-Pd precursor structure compared to the electron-withdrawing $-NO_2$ group at the improper *meta* position and electronically neutral phenyl ring.

Table s5. Optimizations for the Mizoroki-Heck cross-coupling reaction[a]

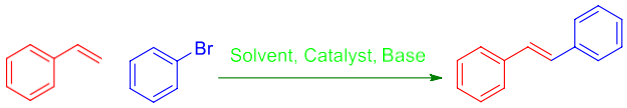

Entry	Base	Cat. Loading(mmol)	Solvent	T (°C)	Yield
1	K_2CO_3	0.05	DMF	130	83
2	K_2CO_3	0.005	DMF	130	80
3	K_2CO_3	0.001	DMF	130	48
4	K_2CO_3	-	DMF	130	-
5	K_2CO_3	0.1	DMF	130	90
6	K_2CO_3	0.005	NMP	130	80
7	K_2CO_3	0.005	Ethanol	75	72
8	K_2CO_3	0.005	H_2O	100	58
9	K_2CO_3	0.005	Toluene	110	46
10	K_2CO_3	0.005	Hexane	80	40
11	Na_2CO_3	0.005	DMF	130	70
12	Cs_2CO_3	0.005	DMF	130	89
13	NaOAc	0.005	DMF	130	57
14	NEt_3	0.005	DMF	130	40
15	Pyridine	0.005	DMF	130	43
16	Cs_2CO_3	0.005	DMF	25	55
17	Cs_2CO_3	0.005	DMF	60	67
18	Cs_2CO_3	0.005	DMF	90	78
19[c]	Cs_2CO_3	0.005	DMF	130	76
20[d]	Cs_2CO_3	0.005	DMF	130	82

[a]Reaction conditions for Mizoroki-Heck cross-coupling reaction: bromobenzene (0.5 mmol), styrene (0.75 mmol), base (1.5 mmol), DMF (2 mL), catalyst **3**, 4 h, in the air.
[b] Catalyst **1**
[c] Catalyst **2**

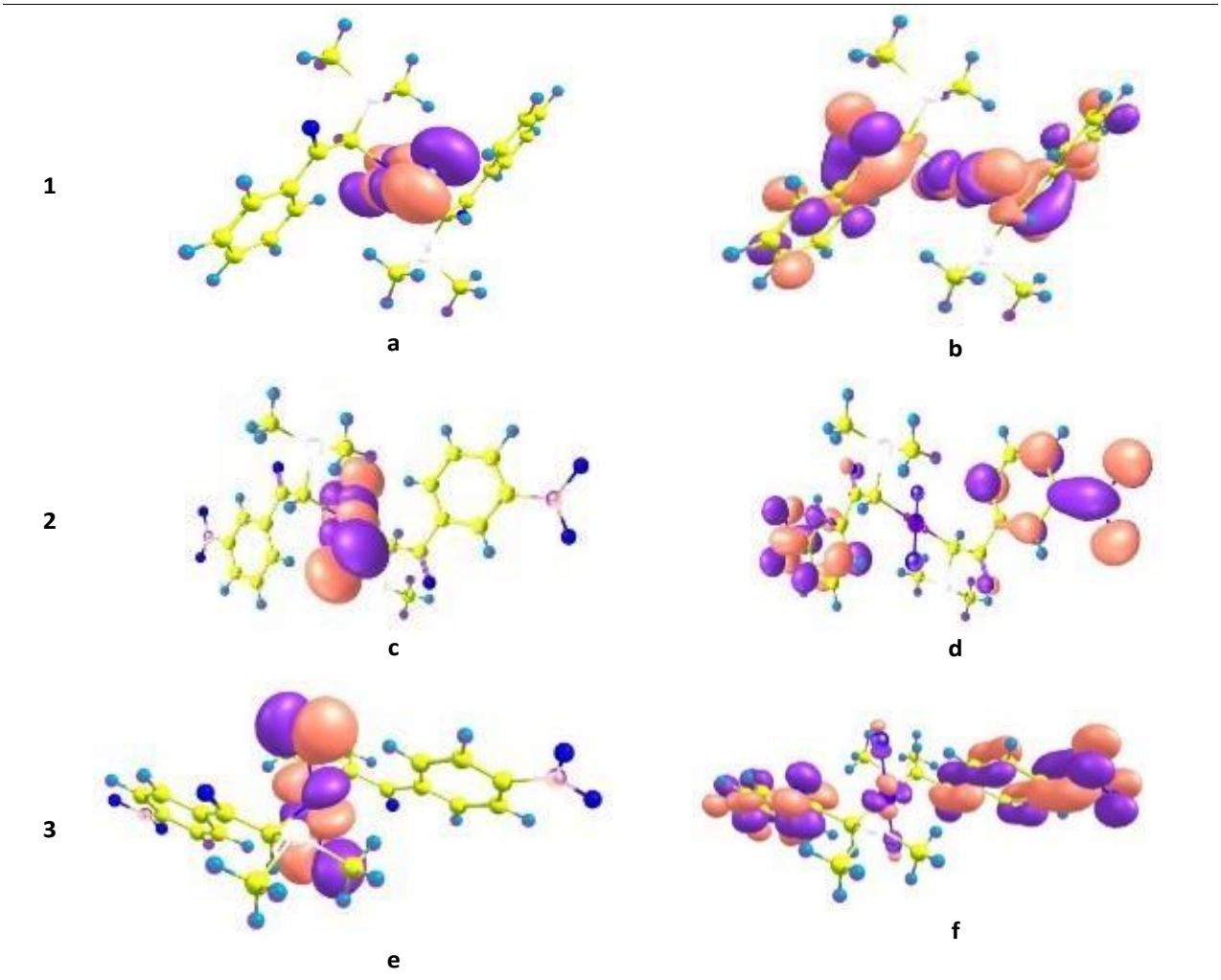

Fig. s1. Illustration of calculated HOMO (a, c, and e) and LUMO (b, d, and f) molecular orbitals for complexes 1-3, respectively

SEM Images of recovered catalyst

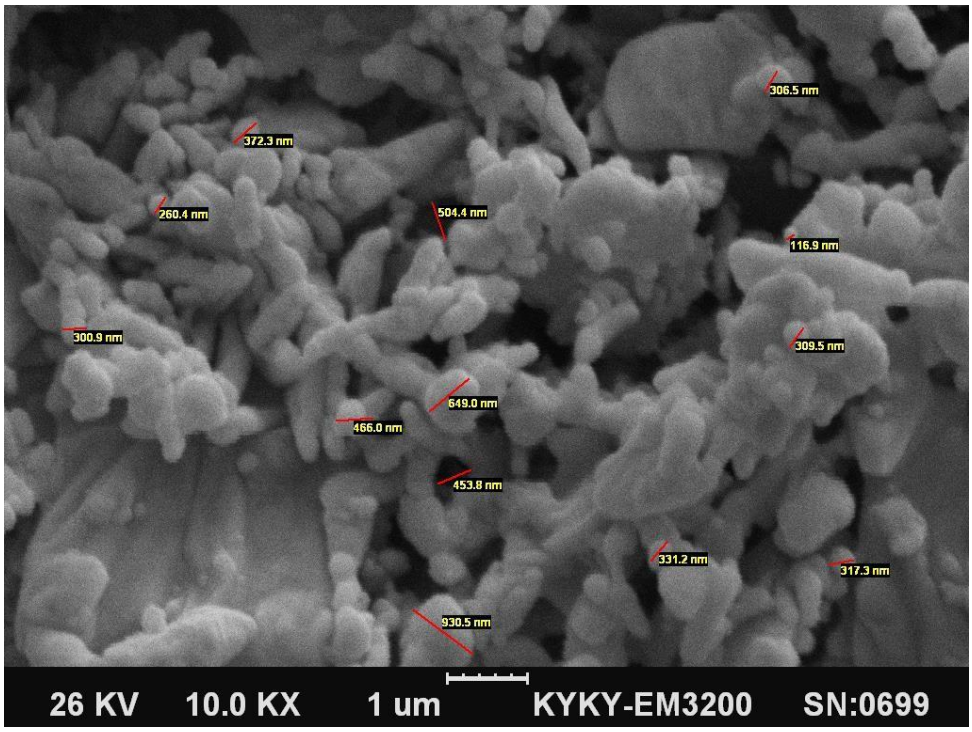

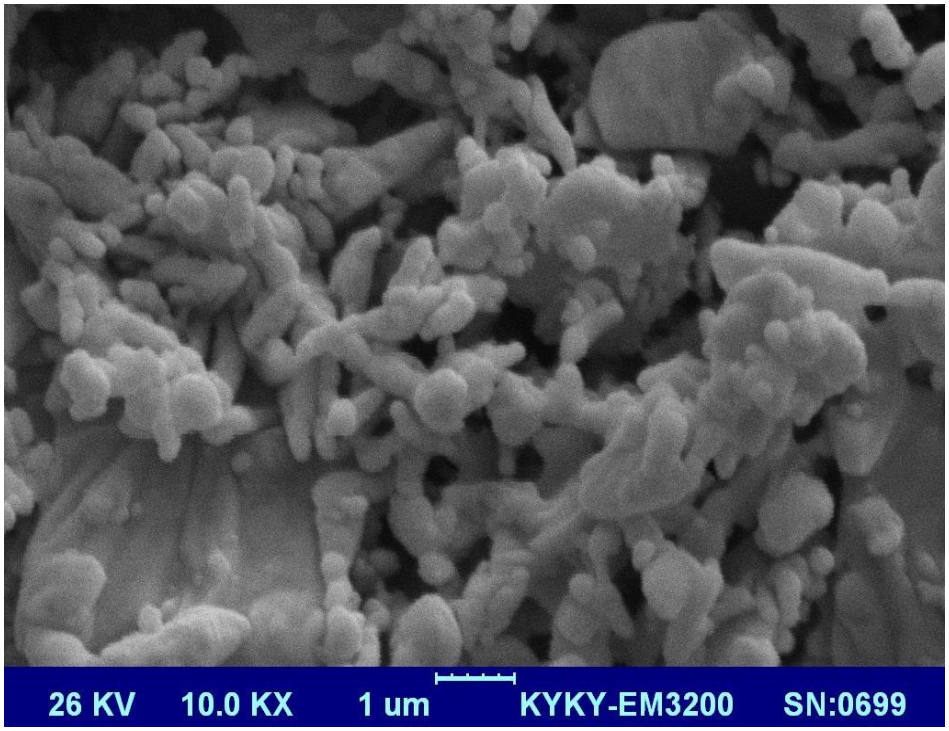

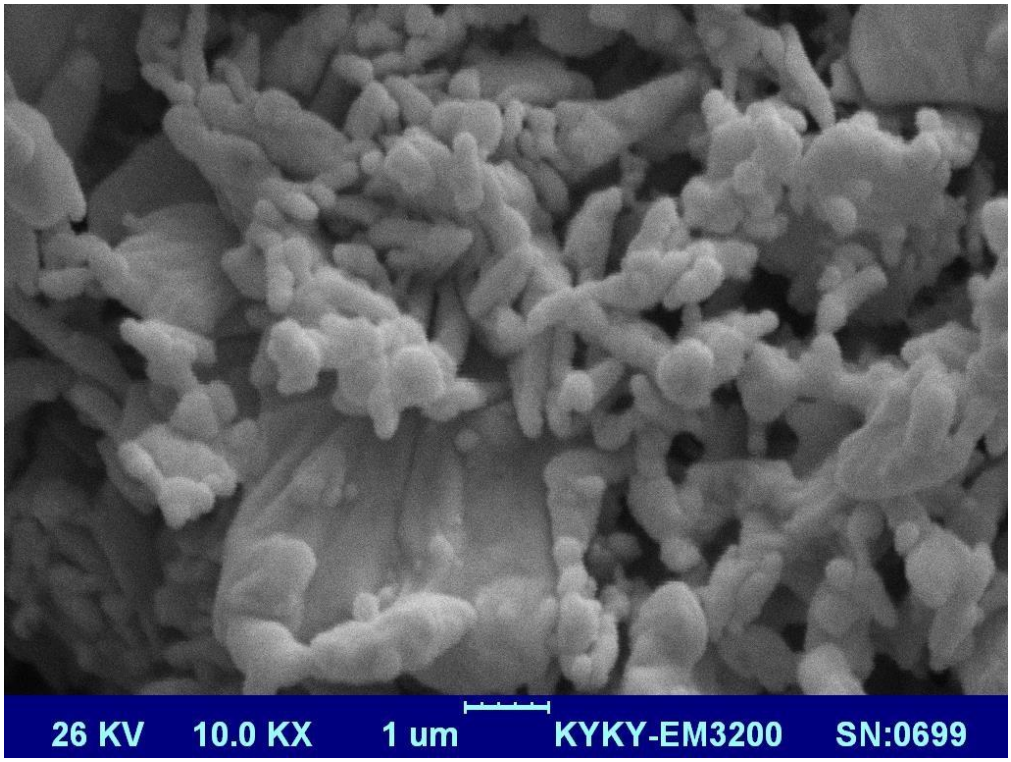
26 KV
10.0 KX
1 um
KYKY-EM3200
SN:0699

Characterization of Mizoroki-Heck reaction products

Data for (E)-1,2-Diphenylethene (1g)
M.p. 121–122 °C. ^{1}H NMR (500.13 MHz, $CDCl_3$) δ_H (ppm): δ = 7.10 (s, 2H), 7.24 (t, 2H), 7.34 (t, 4H), 7.49 (d, 4H). ^{13}C NMR (125.77 MHz, $CDCl_3$) δ_C (ppm): δ = 127.00, 128.09, 128.16, 128.81 [1].

Data for (E)-1-Methyl-4-styrylbenzene (2g)
M.p. 114–116 °C. ^{1}H NMR (89.60 MHz, $CDCl_3$) δ_H (ppm): δ = 2.39 (s, 3H), 6.88–7.87(m, 11H). ^{13}C NMR (62.90 MHz, $CDCl_3$) δ_C (ppm): δ = 21.29, 126.79, 126.87, 127.82, 127.87, 128.78, 129.11, 129.75, 134.68, 134.56, 137.48, 137.61 [2].

Data for trans-4-methoxystilbene (3g)
M.p.134-136 °C. ^{1}H NMR (400.61 MHz, $CDCl_3$) δ_H (ppm): 3.75 (s, 3H, OCH_3), 6.82-7.43 (m, 11H). ^{13}C NMR (100.62 MHz, $CDCl_3$) δ_C (ppm): 159.32, 137.66, 130.16, 128.64, 128.22, 127.72, 127.21, 126.63, 126.25, 114.14, 55.34 (s, OCH_3) [3].

Data for (E)-1-nitro-4-styrylbenzene (4g)
M.p. 156–157 °C. ^{1}H NMR (500.13 MHz, CDCl3) δH (ppm): δ = 8.21 (d, 2H), 7.13–7.64 (m, 9H). ^{13}C NMR (125.77 MHz, $CDCl_3$) δ_C (ppm): δ = 124.60, 125.71, 127.30, 129.30, 133.74, 144.26, 147.17 [1-3].

Data for (E)-1-(4-styryl-phenyl)aldehyde (5g)
M.p. 110-112 °C. ^{1}H NMR (500.13 MHz, $CDCl_3$) δ_H (ppm): 7.13-8.04 (m, 11H), 10.05 (s, 1H, CHO). ^{13}C NMR (125.77 MHz, $CDCl_3$) δ_C (ppm): 192.74 (s, CO), 138.82, 137.28, 137.16, 132.75, 130.99, 129.81, 129.28, 129.23, 128.60, 127.64, 127.54, 127.14 [1-3].

Data for (E)-1-methyl-4-styrylbenzoate (6g)
M.p. 158 °C. ^{1}H NMR (89.60 MHz, $CDCl_3$) δ_H (ppm): 2.58 (s, 3H), 6.81–8.53 (m, 7H). ^{13}C NMR (125.77 MHz, $CDCl_3$) δ_C (ppm): 27.50, 126.61, 126.92, 128.35, 128.82, 128.91, 129.04, 129.77, 130.98, 135.41, 139.59, 196.99 [4].

Data for (E)-1-styrylnaphthalene (7g)
M.p. 70-71 °C. ^{1}H NMR (89.60 MHz, $CDCl_3$) δ_H (ppm): 8.31–8.37 (br, 1H), 7.18-8.12 (m, 13H). ^{13}C NMR (125.77 MHz, $CDCl_3$) δ_C (ppm): 116.34, 123.71, 123.86, 125.79, 125.87, 125.92, 126.18, 126.78, 127.87, 128.13, 128.71, 128.84, 131.83 [5].

Data for Ethyl 3-phenylacrylate (8g)
Light yellow liquid. ^{1}H NMR (500.13 MHz, $CDCl_3$) δ_H(ppm) = 7.66 (d, 1H, J = 16.10 Hz), 7.24–7.65 (m, 5H), 6.41 (d, 1H), 4.24 (q, 2H), 1.23 (t, 3H). ^{13}C NMR (125.77 MHz, $CDCl_3$) δ_C (ppm): 167.39 (s, CO), 144.99, 134.90, 130.62, 129.29, 129.25, 128.45, 118.72, 60.91 (s, CH_2), 14.77 (s, CH_3) [6].

Data for (E)-Ethyl 3-(4-nitrophenyl)acrylate (9g)
M.p. 135-136 °C. ^{1}H NMR (500.13 MHz, $CDCl_3$) δ_H (ppm): 1.33 (t, 3H, CH_3), 4.27 (q, 2H, CH_2), 6.53 (s, 1H), 7.65 (q, 2H), 8.23 (d, 2H). ^{13}C NMR (127.77 MHz, $CDCl_3$) δ_C (ppm): 166.44 (s, CO), 148.92, 142.03, 141.03, 129.04, 124.61, 123.04, 61.44 (s, CH_2), 14.70 (s, CH_3) [7].

Data for ethyl (E)-3-(p-tolyl)acrylate (10g)

Light brown liquid, ^{1}H NMR (89.60 MHz, $CDCl_3$) δ_H (ppm): 7.66 (d, 1H, *J* = 16.21 Hz), 7.13–7.47 (m, 4H), 6.38 (d, 1H, *J* = 16.03 Hz), 4.26 (q, 2H, *J* = 7.07 Hz), 2.37 (s, 3H), 1.33 (t, 3H, *J* = 6.98 Hz). ^{13}C NMR (100.62 MHz, $CDCl_3$) δ_C (ppm): 167.2 (s, CO), 144.5, 140.6, 131.7, 129.6, 128.0, 117.1, 60.4 (s, CH_2), 21.4 (s, CH_3), 14.3 (s, CH_3). [8]

Data for ethyl (E)-3-(naphthalen-1-yl)acrylate (11g)

Yellow liquid^{1}H NMR (89.60 MHz, $CDCl_3$) δ_H (ppm): 8.37 (d, 1H, *J* = 15.68 Hz), 7.17–8.07 (m, 7H), 6.35 (d, 1H, *J* = 15.77 Hz), 4.16 (q, 2H, *J* = 7.07 Hz), 1.21 (t, 3H, *J* = 7.07 Hz). ^{13}C NMR (100.62 MHz, $CDCl_3$) δ_C (ppm): 165.7 (s, CO), 140.4, 132.5, 130.6, 130.2, 129.3, 127.5, 125.7, 125.0, 124.3, 123.8, 122.2, 119.7, 59.4 (s, CH_2), 13.2 (s, CH_3) [9].

Data for Ethyl 3-(4-formylphenyl)acrylate (12g)

Light yellow liquid. ^{1}H NMR (89.60 MHz, $CDCl_3$) δ_H (ppm): δ = 10.20 (s, 1H), 8.35 (d, 1H), 7.11–7.88 (m, 4H), 6.20 (d, 1H), 4.16 (2H), 1.92 (t, 3H). ^{13}C NMR (62.90 MHz, $CDCl_3$) (ppm) (ppm): δ = 191.76 (s, CO), 166.56 (s, CO), 142.88, 133.54, 131.00, 129.64, 129.47, 129.09, 128.84, 120.11, 60.70 (s, CH_2), 14.09 (s, CH_3) [10].

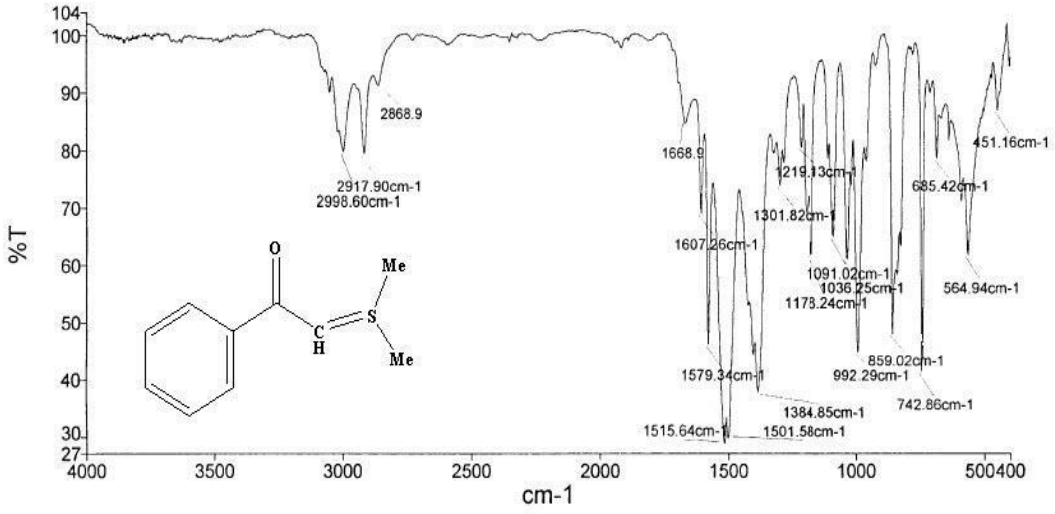

Spectra 1: IR of Y1

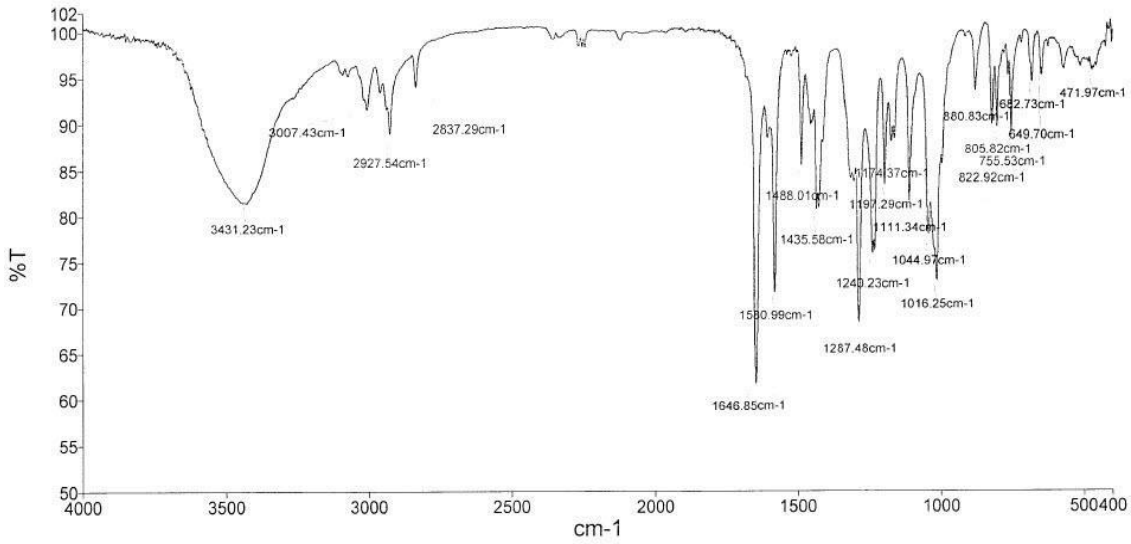

Spectra 2: IR of compound 1

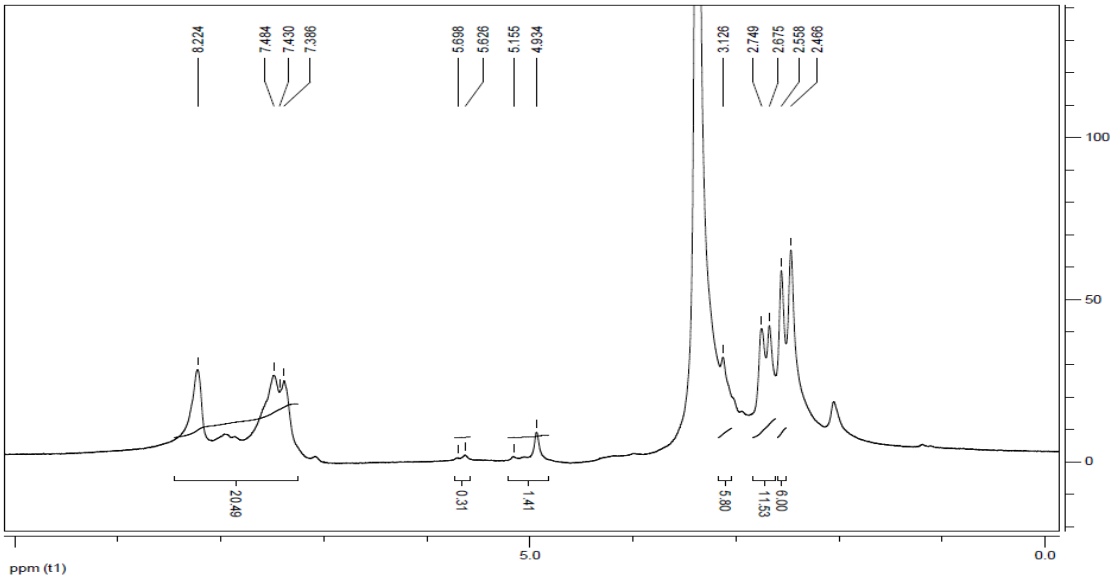

Spectra 3: [1]H NMR of compound 1

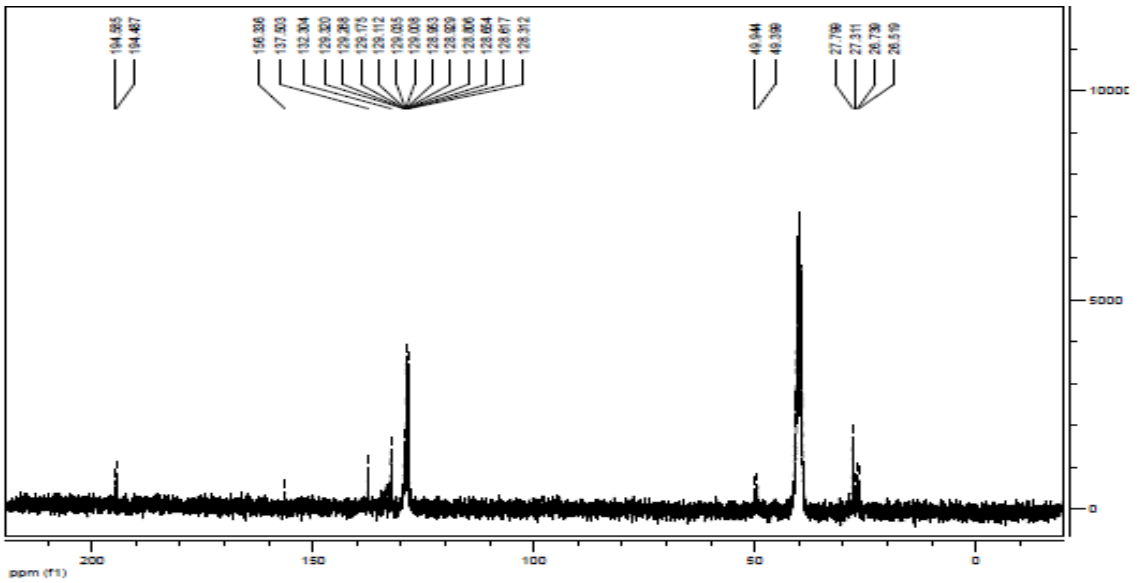

Spectra 4: [13]C NMR of compound 1

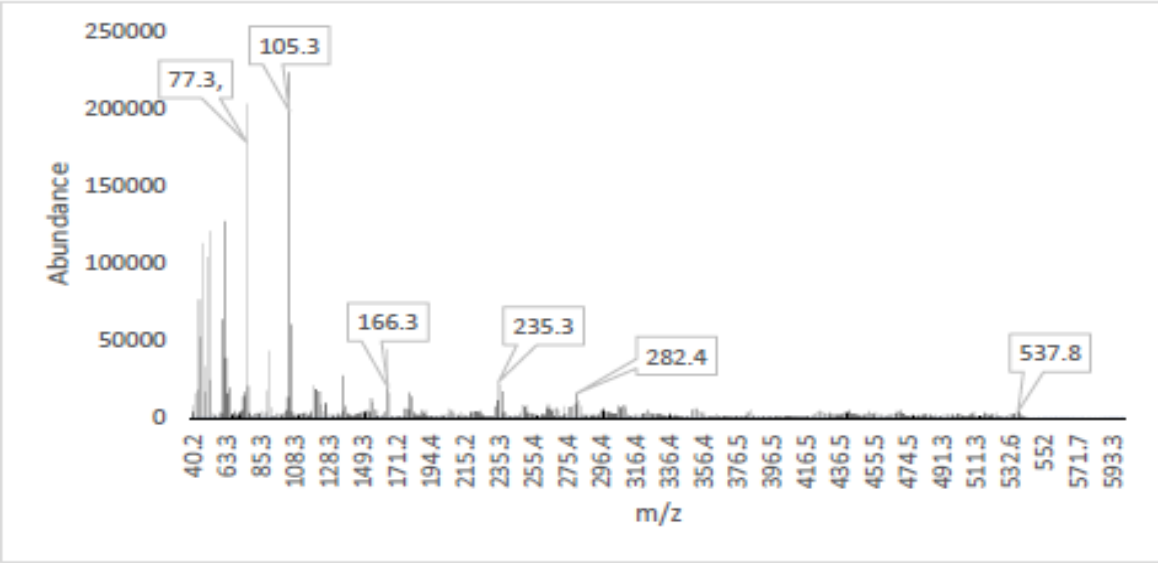

Spectra 5: MS analysis of compound 1

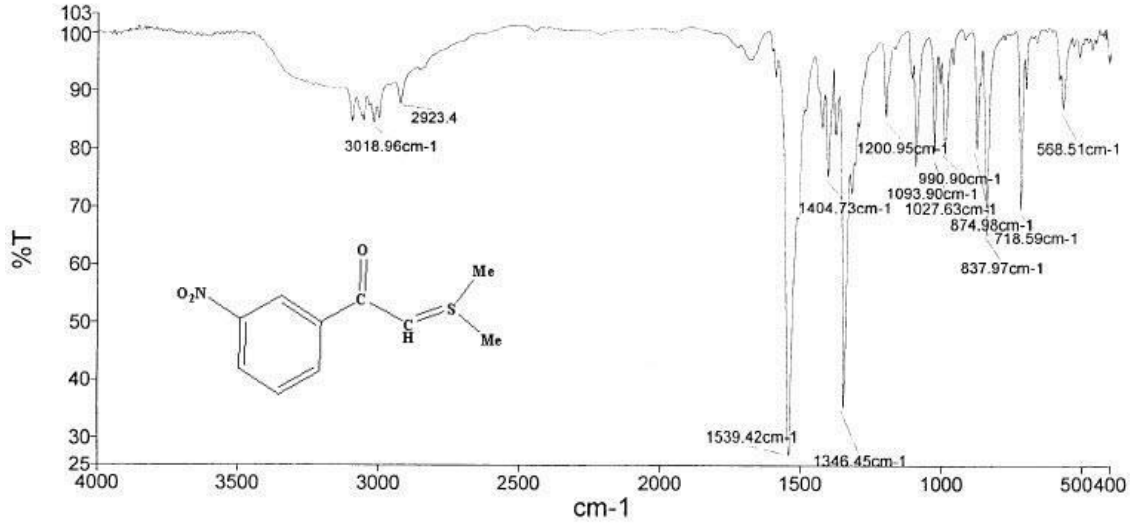

Spectra 6: IR of Y2

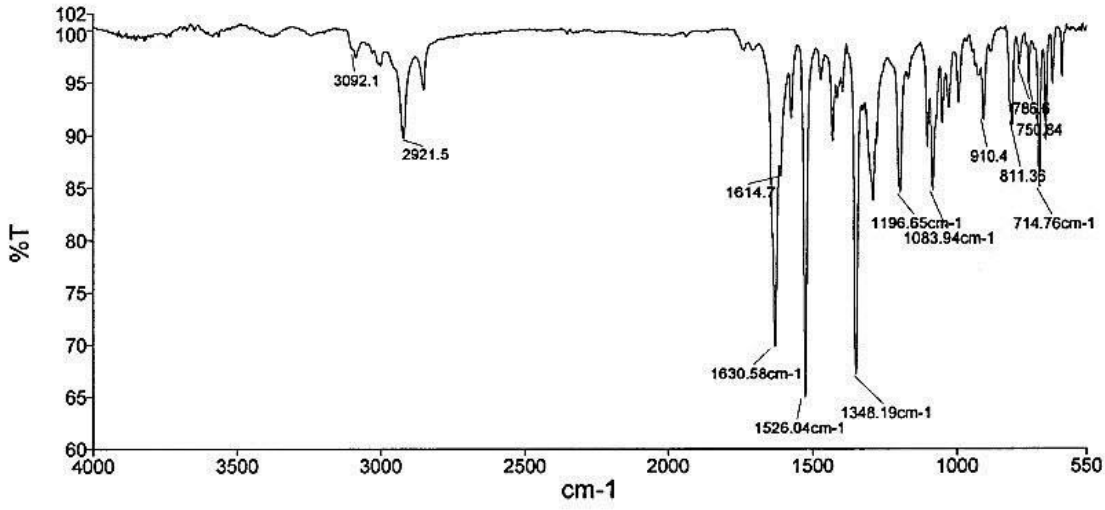

Spectra 7: IR of compound 2

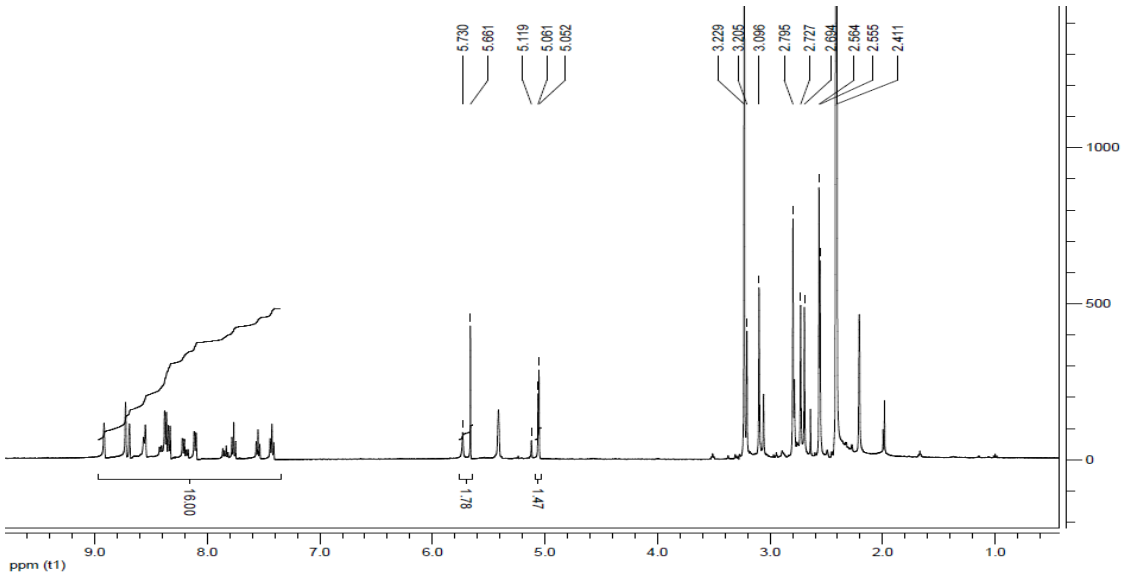

Spectra 8: [1]HNMR of compound 2

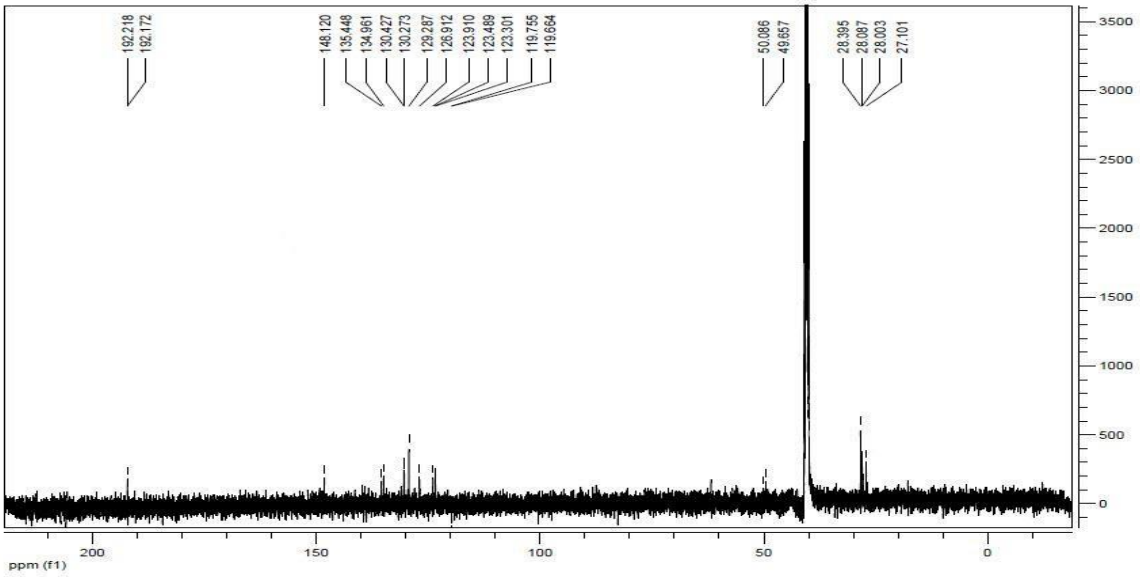

Spectra 9: ^{13}C NMR of compound 2

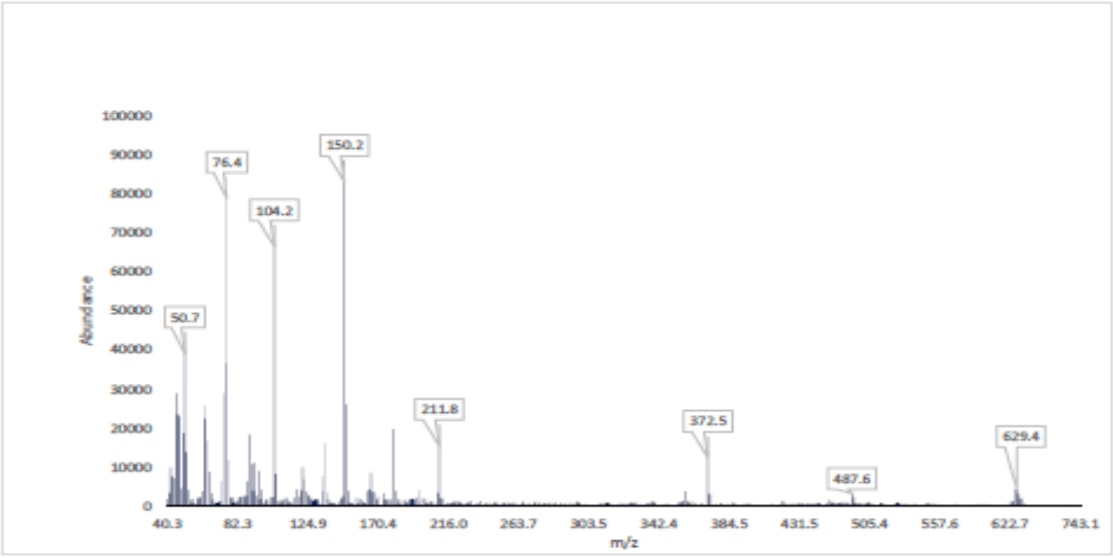

Spectra 10: MS analysis of compound 2

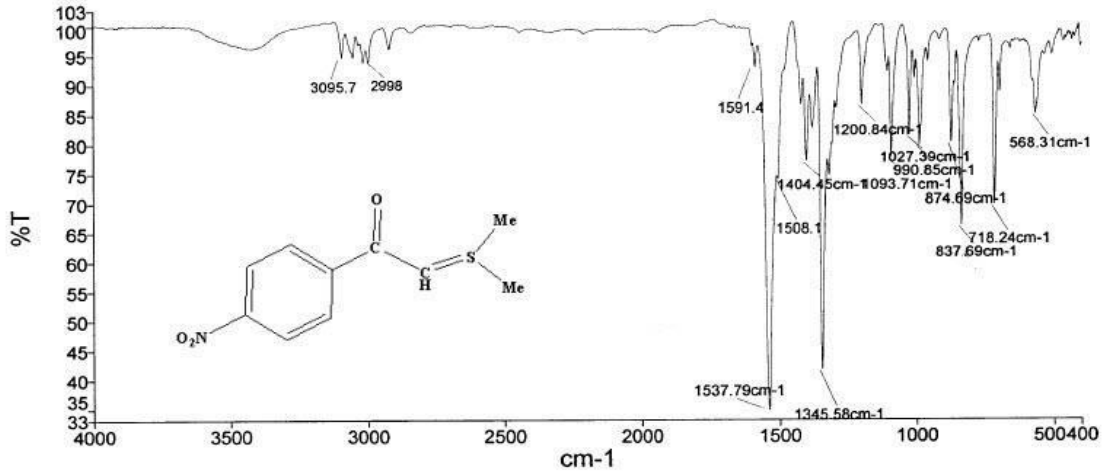

Spectra 11: IR of Y3

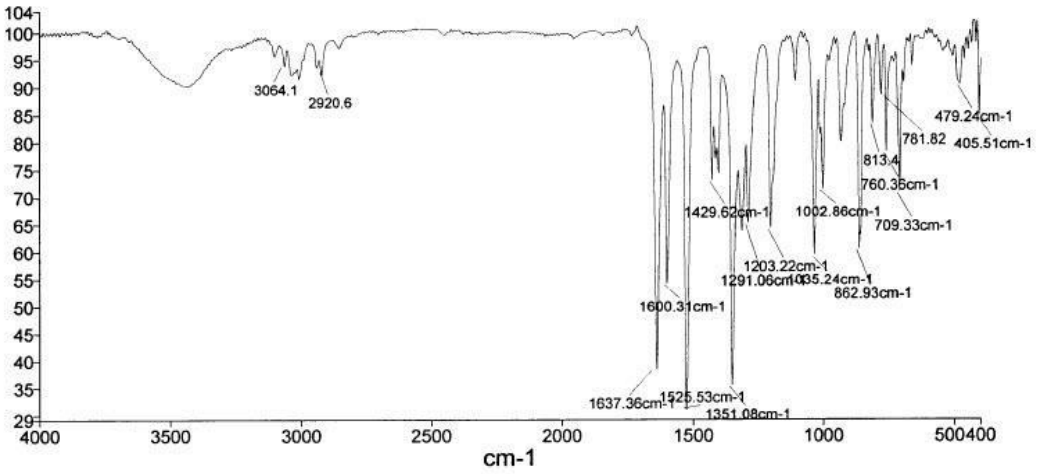

Spectra 12: IR of compound 3

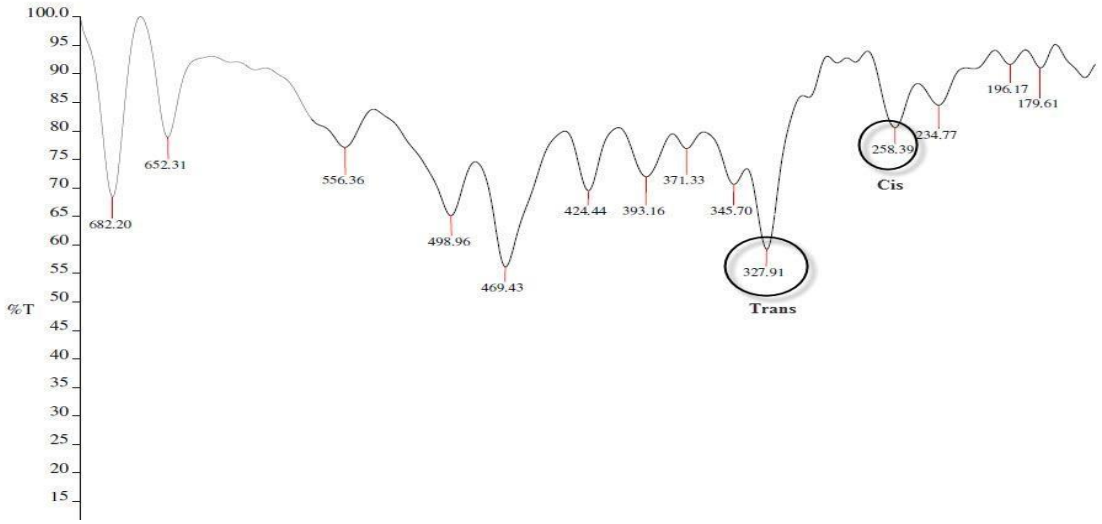

Spectra 13: Far IR of compound 3

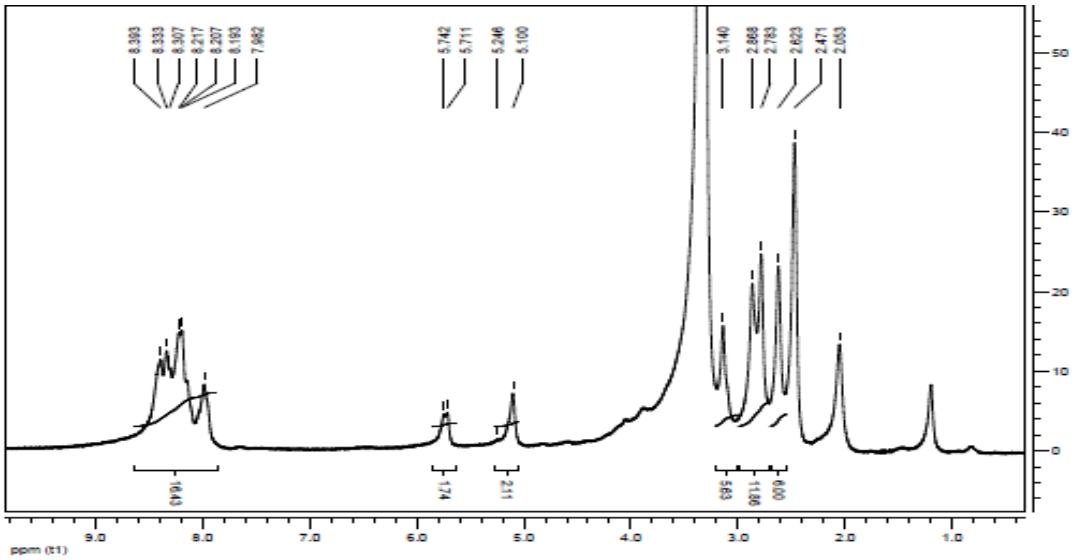

Spectra 14: ^{1}H NMR of compound 3

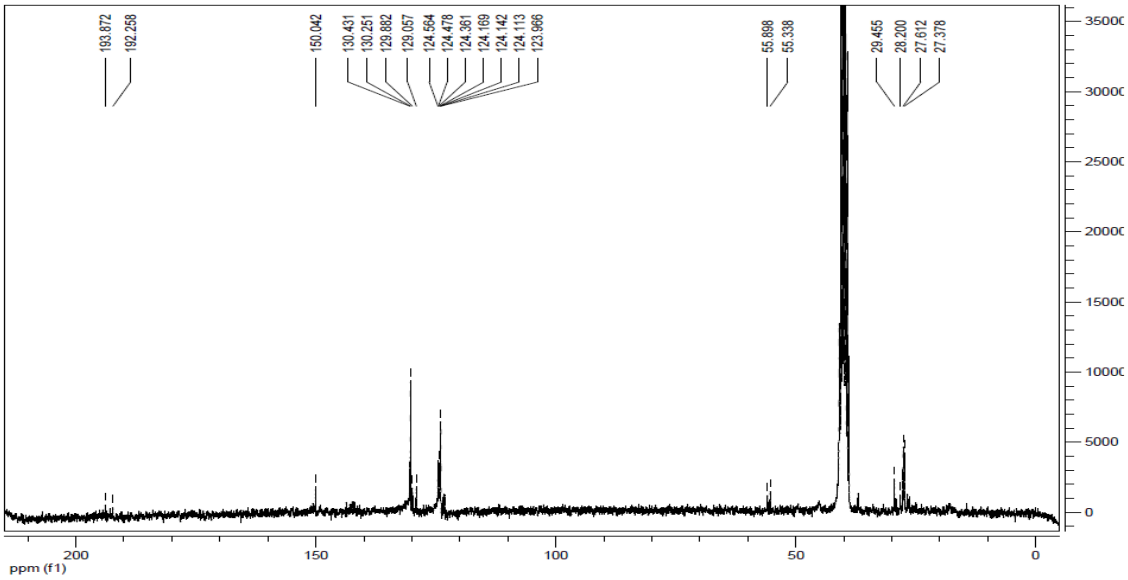

Spectra 15: ^{13}C NMR of compound 3

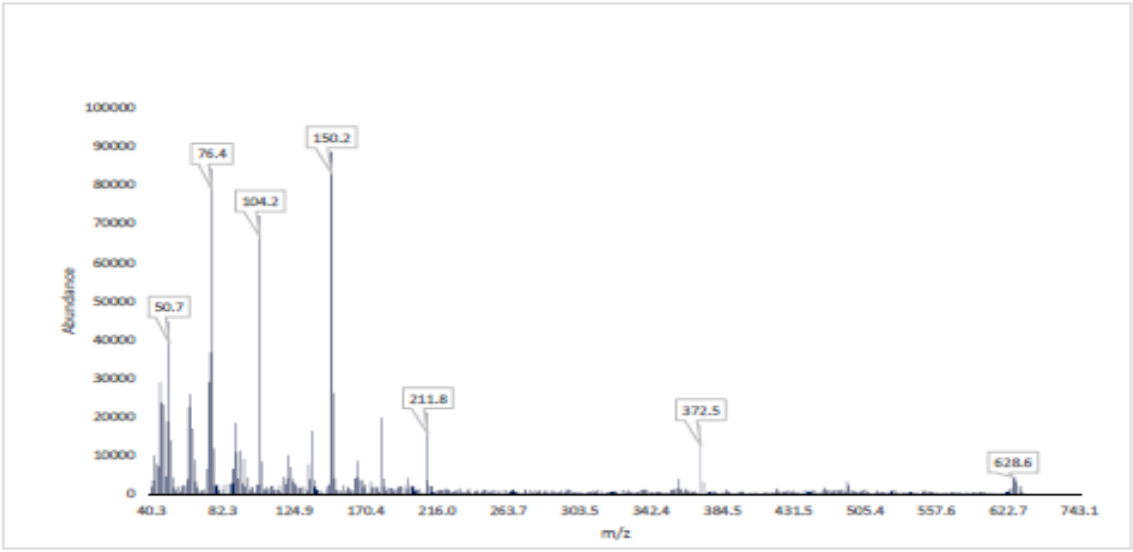

Spectra 16: MS analysis of compound 3

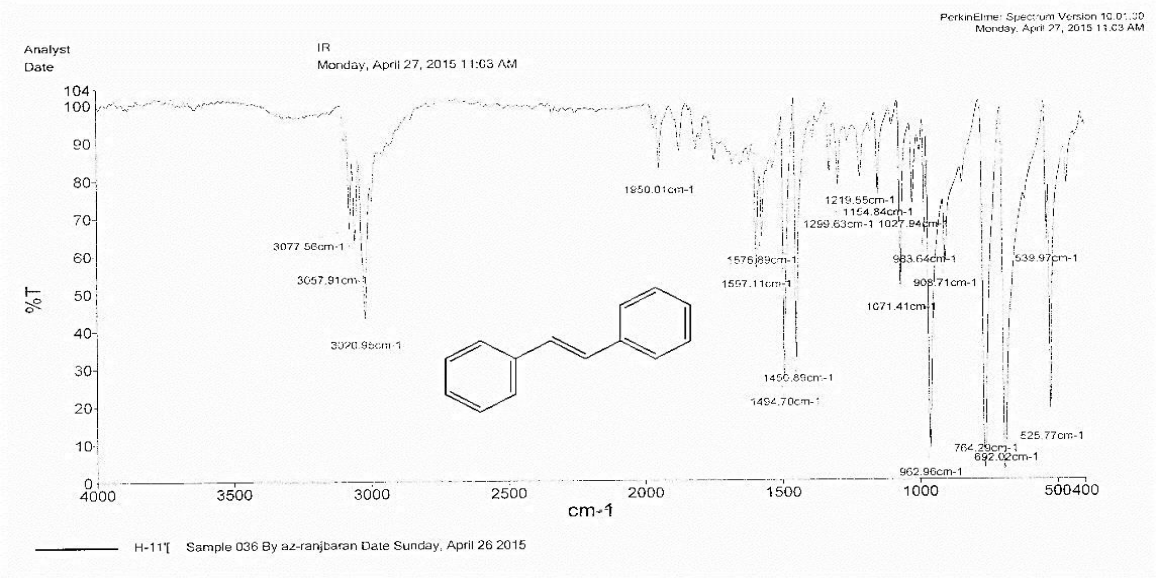

Spectra 17: IR of (1g)

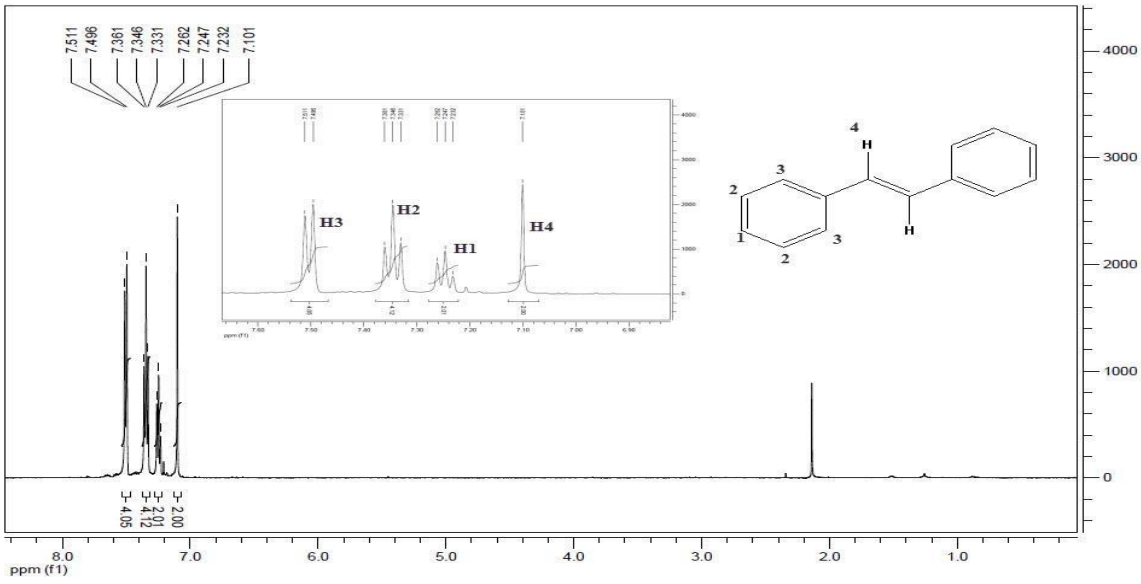

Spectra 18: ^{1}H NMR of (1g)

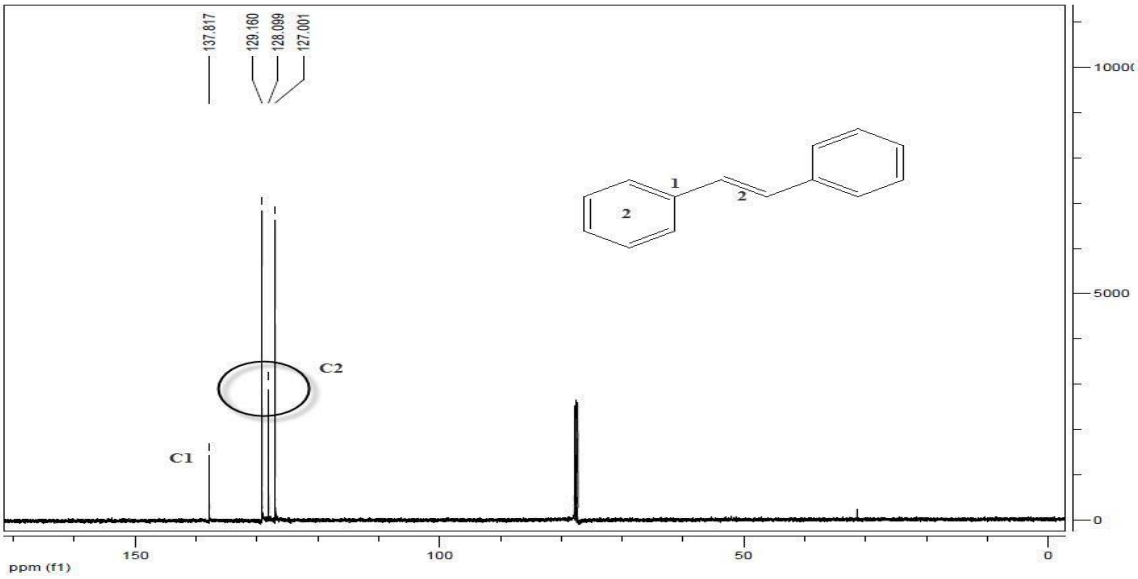

Spectra 19: ^{13}C NMR of (1g)

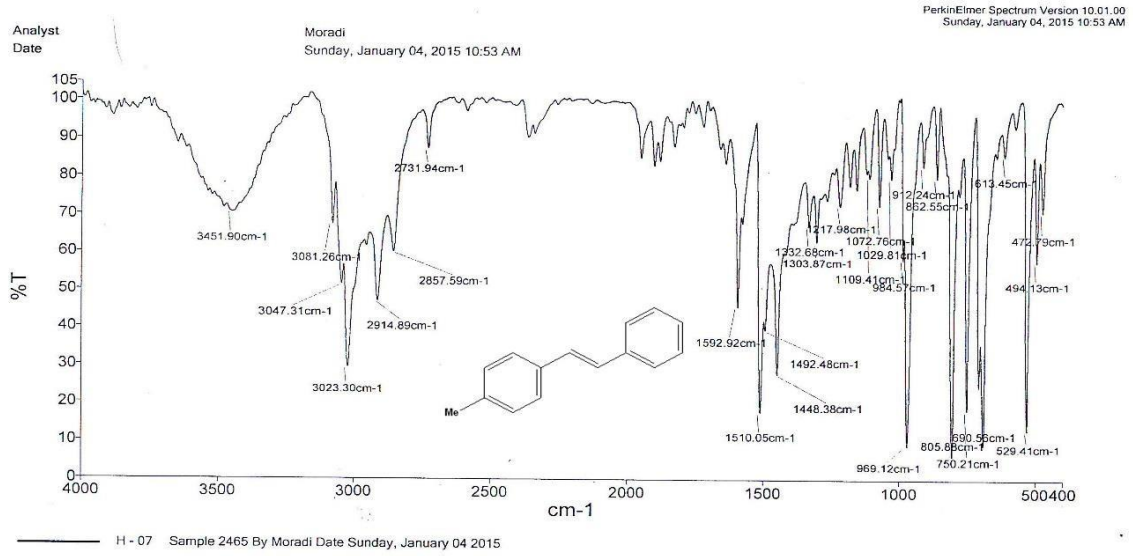

Spectra 20: IR of (2g)

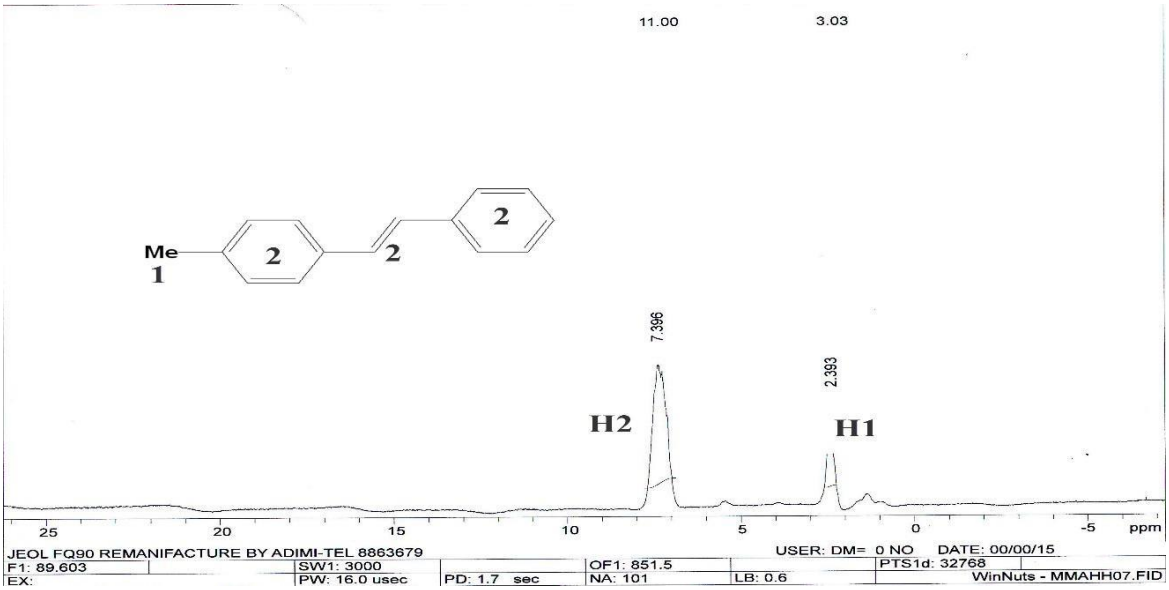

Spectra 21: [1]H NMR of (2g)

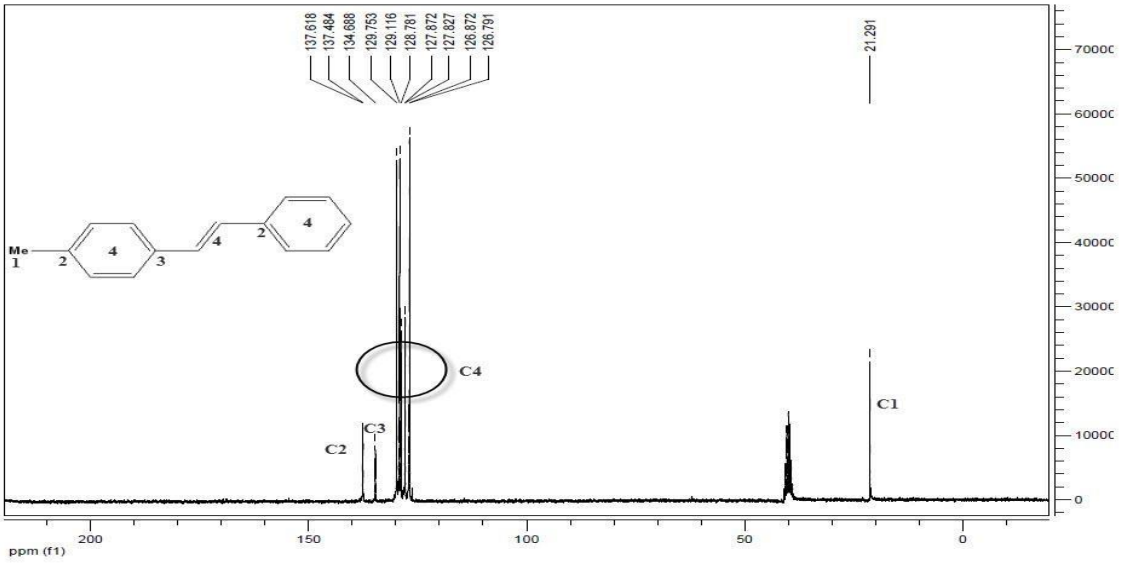

Spectra 22: [13]C NMR of (2g)

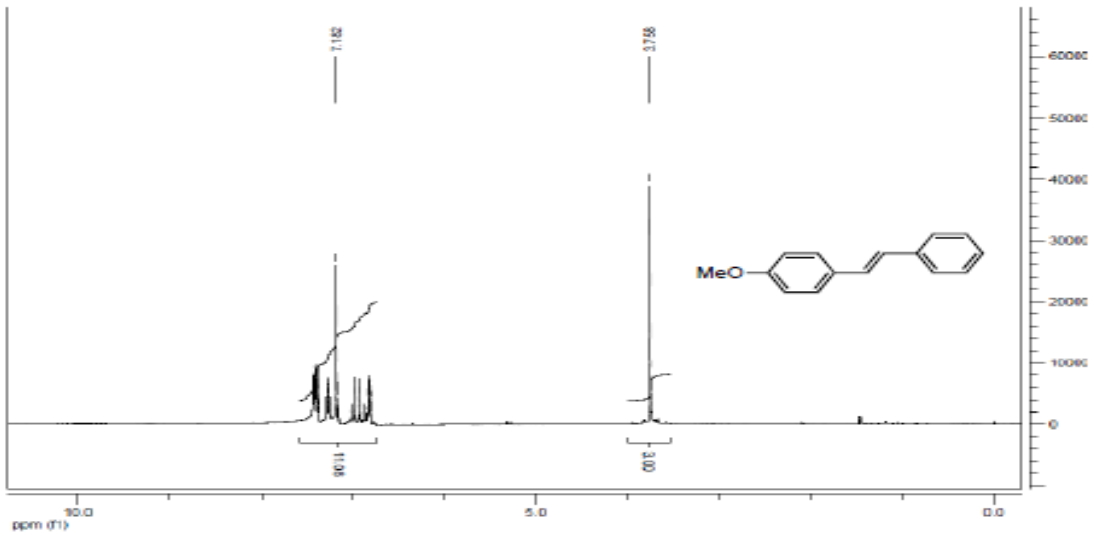

Spectra 23: ^{1}H NMR of (3g)

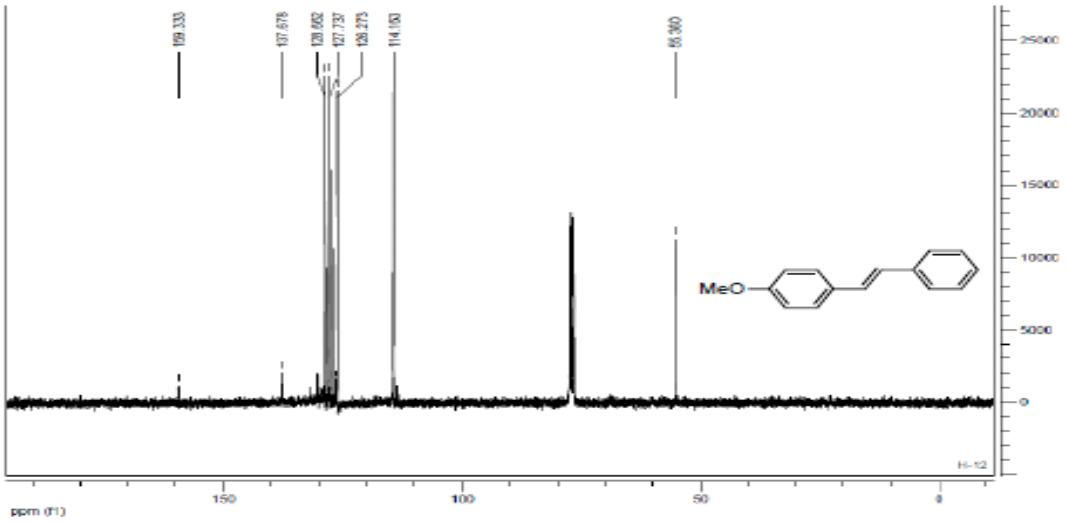

Spectra 24: ^{13}C NMR of (3g)

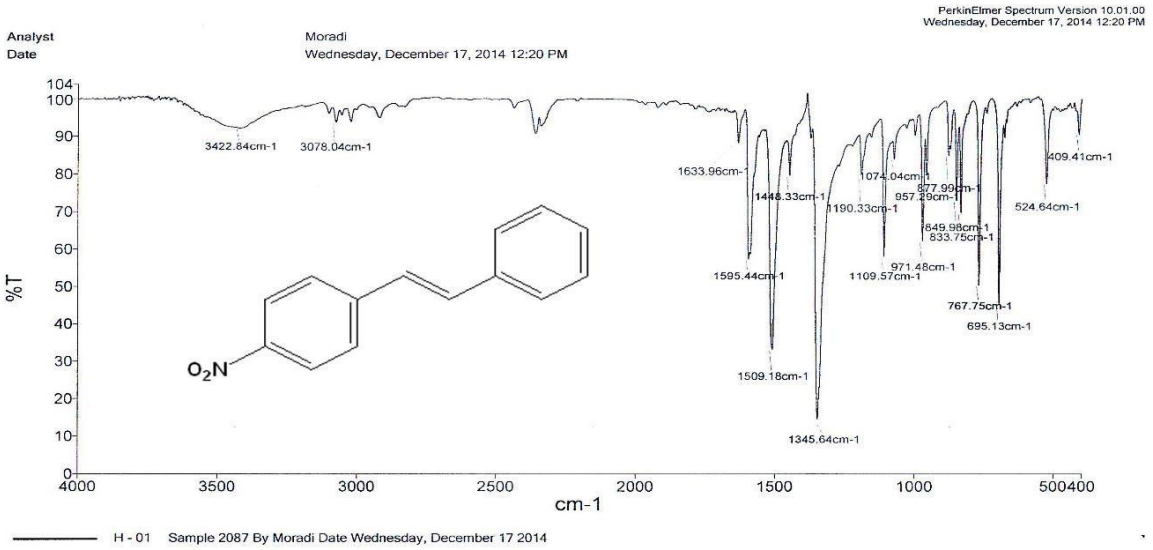

Spectra 25: IR of (4g)

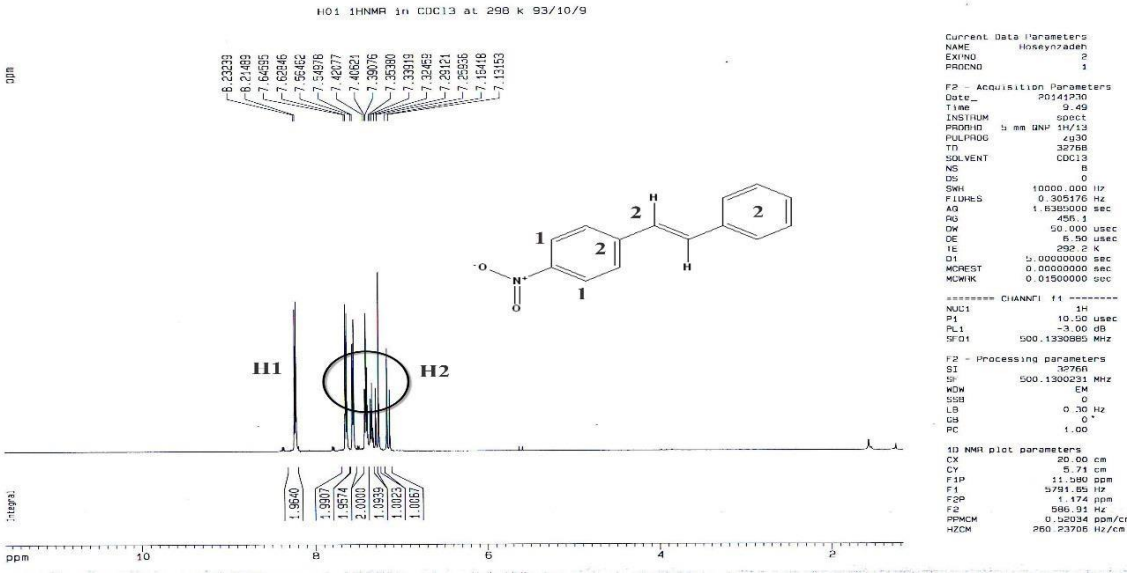

Spectra 26: ^{1}H NMR of (4g)

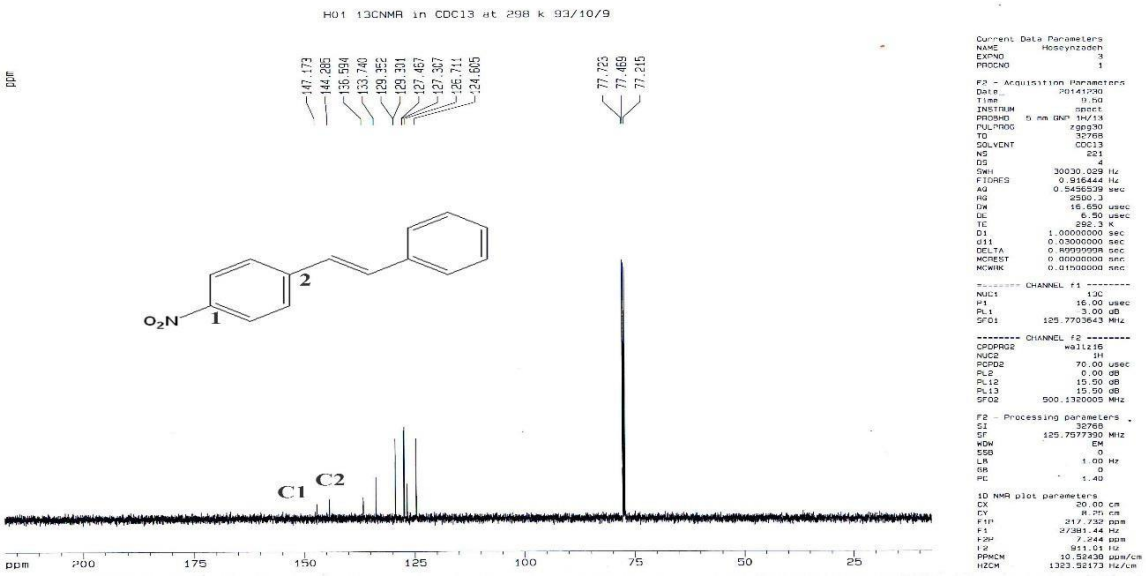

Spectra 27: 13C NMR of (4g)

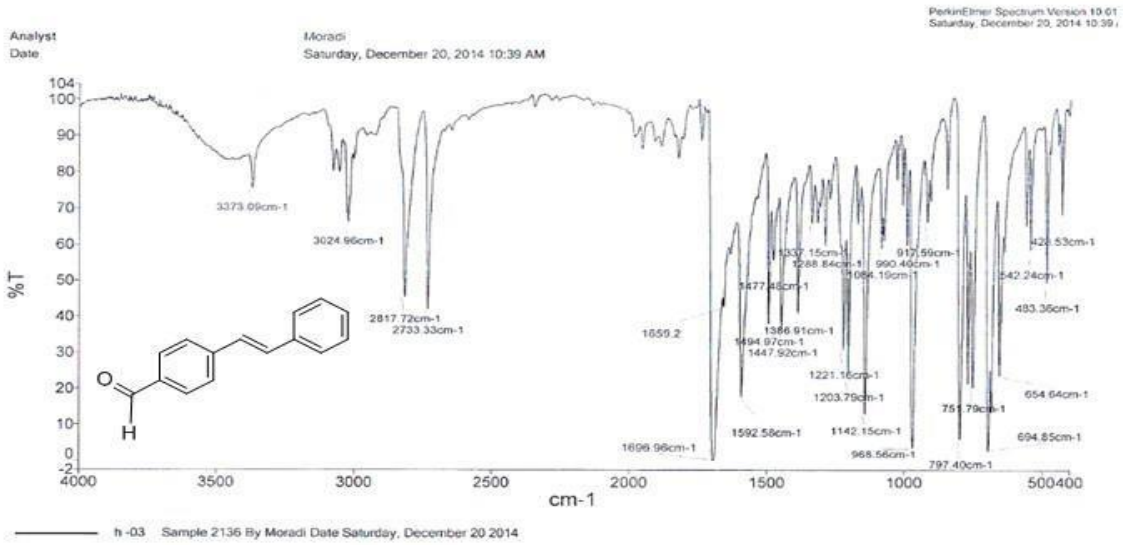

Spectra 28: IR of (5g)

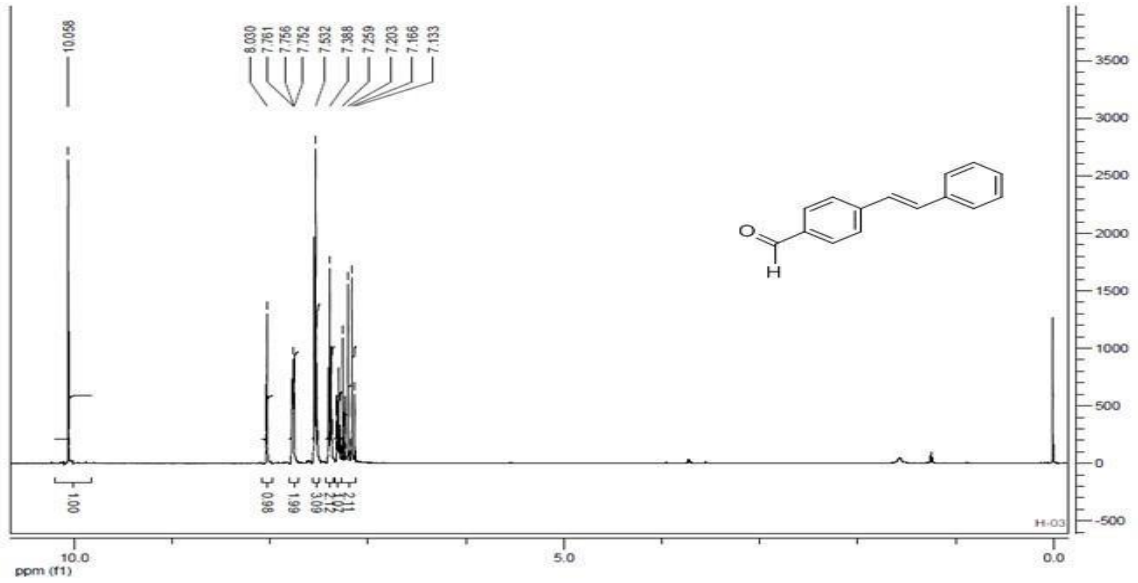

Spectra 29: [1]H NMR of (5g)

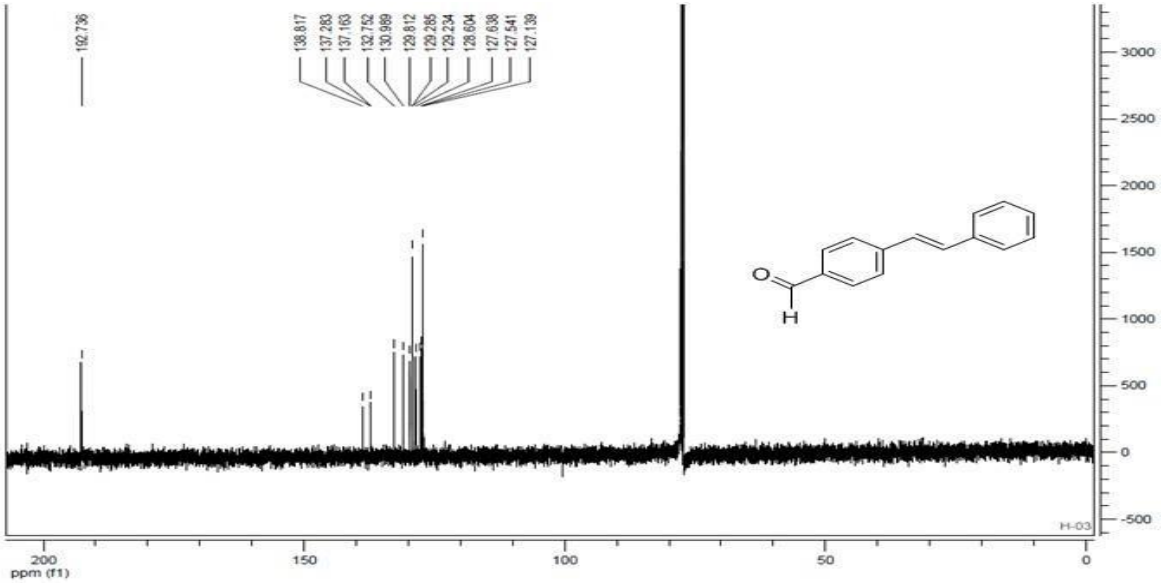

Spectra 30: [13]C NMR of (5g)

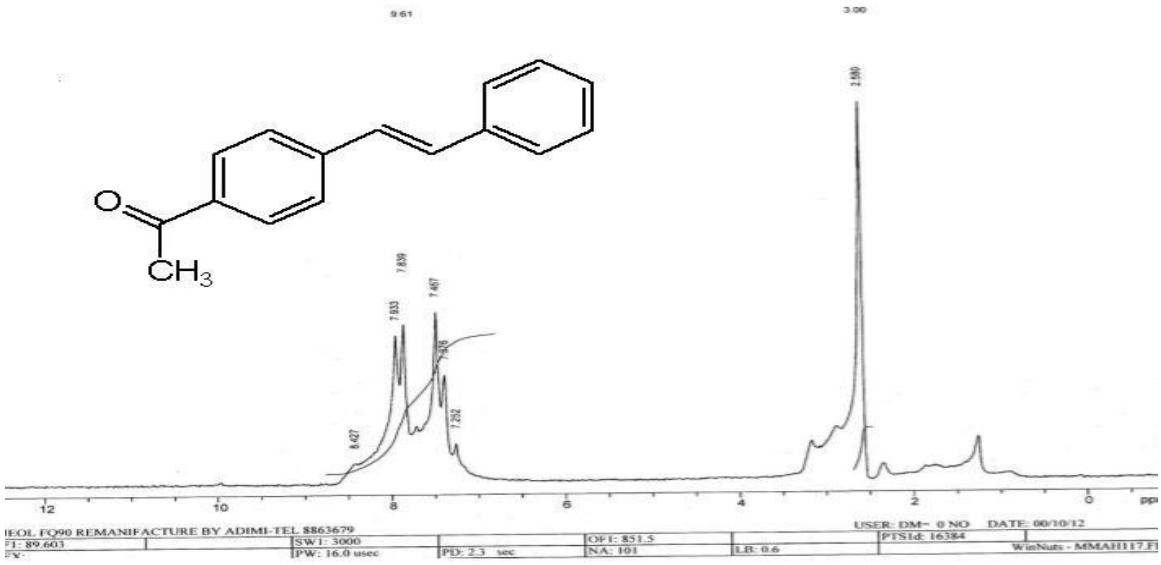

Spectra 31: [1]H NMR of (6g)

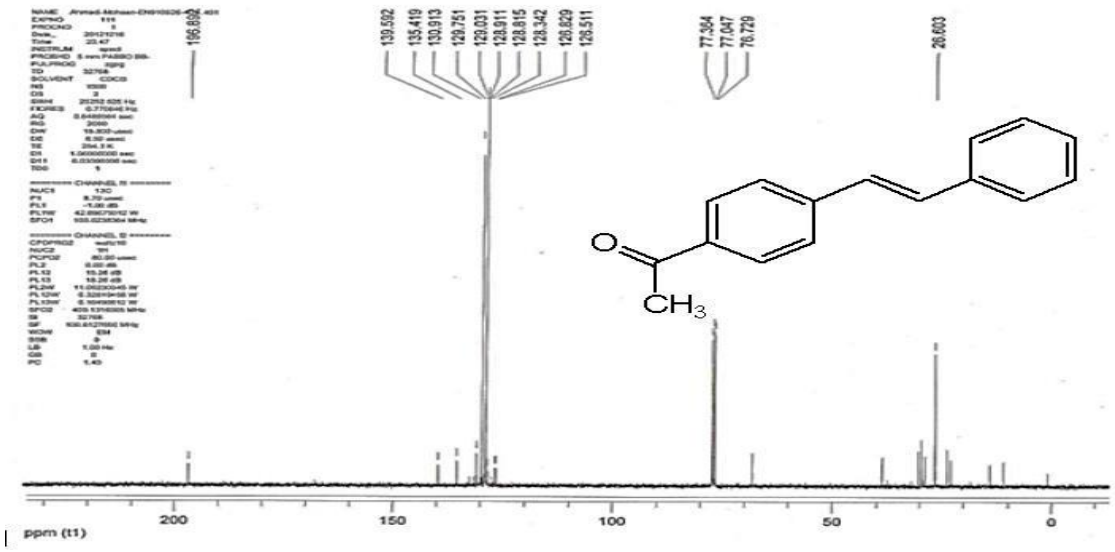

Spectra 32: [13]C NMR of (6g)

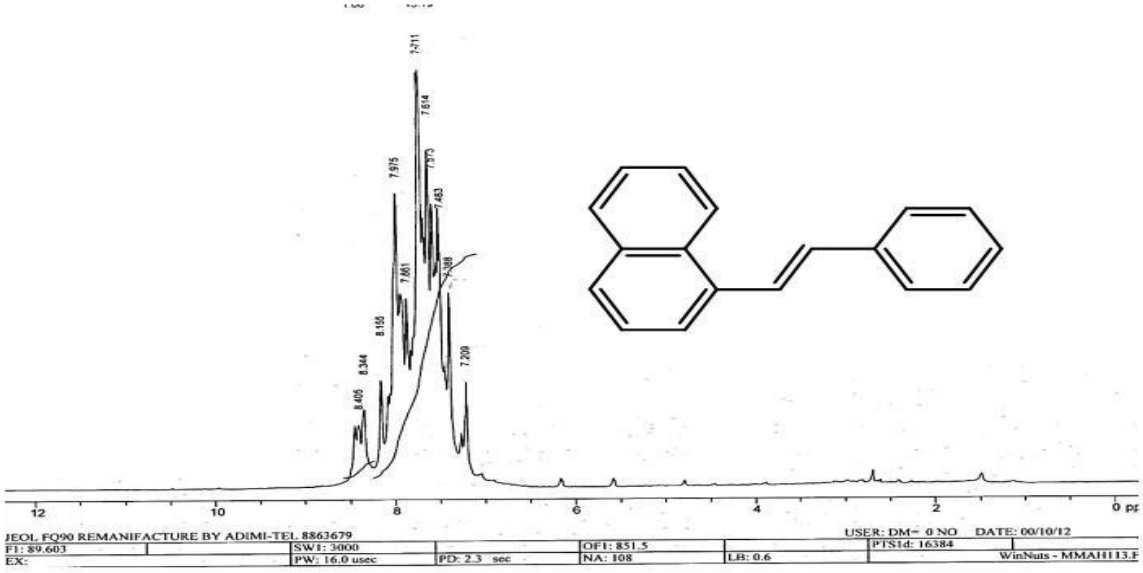

Spectra 33: ^{1}H NMR of (7g)

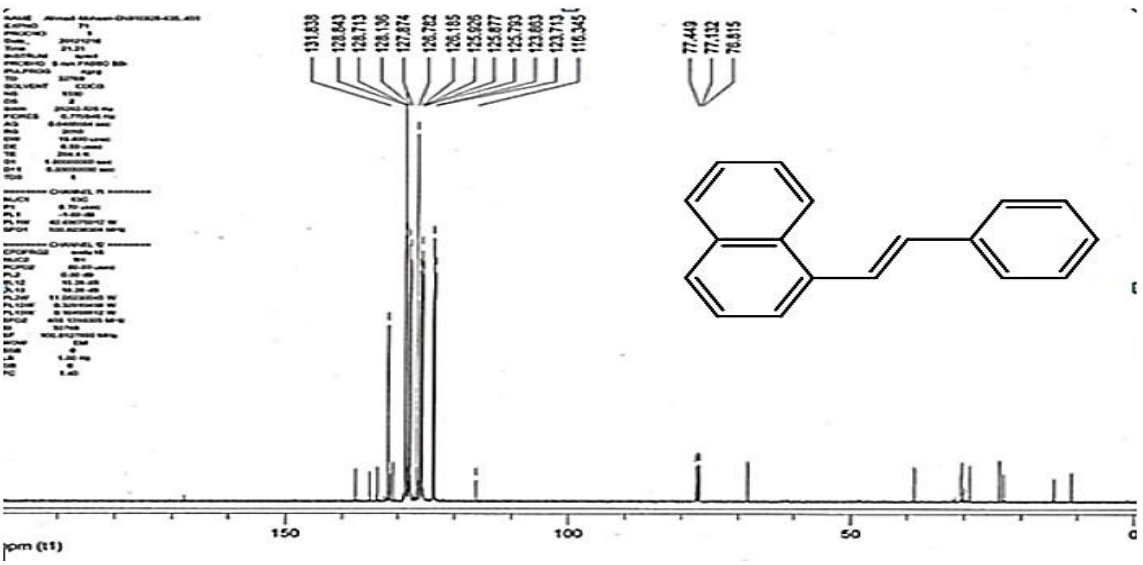

Spectra 34: ^{13}C NMR of (7g)

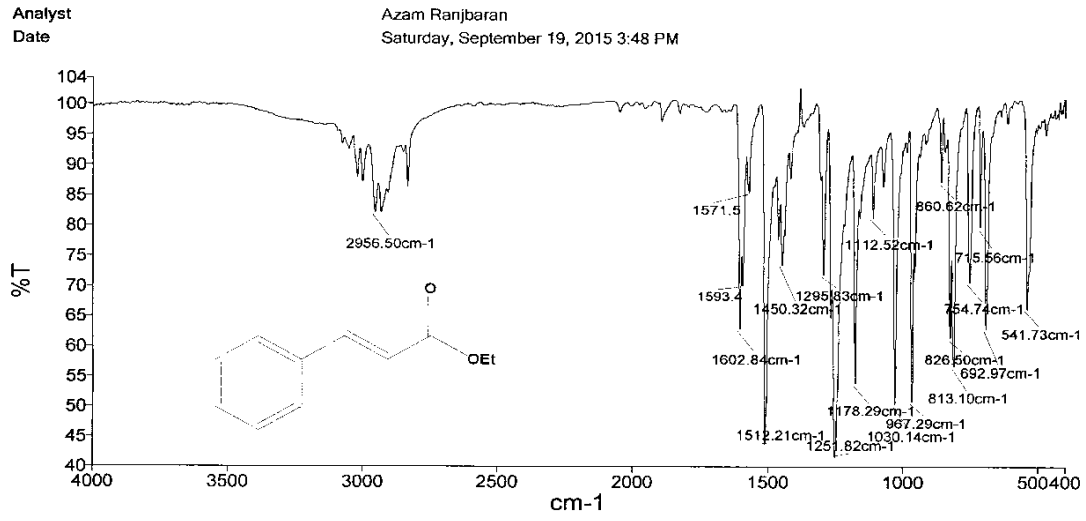

Spectra 35: IR of (8g)

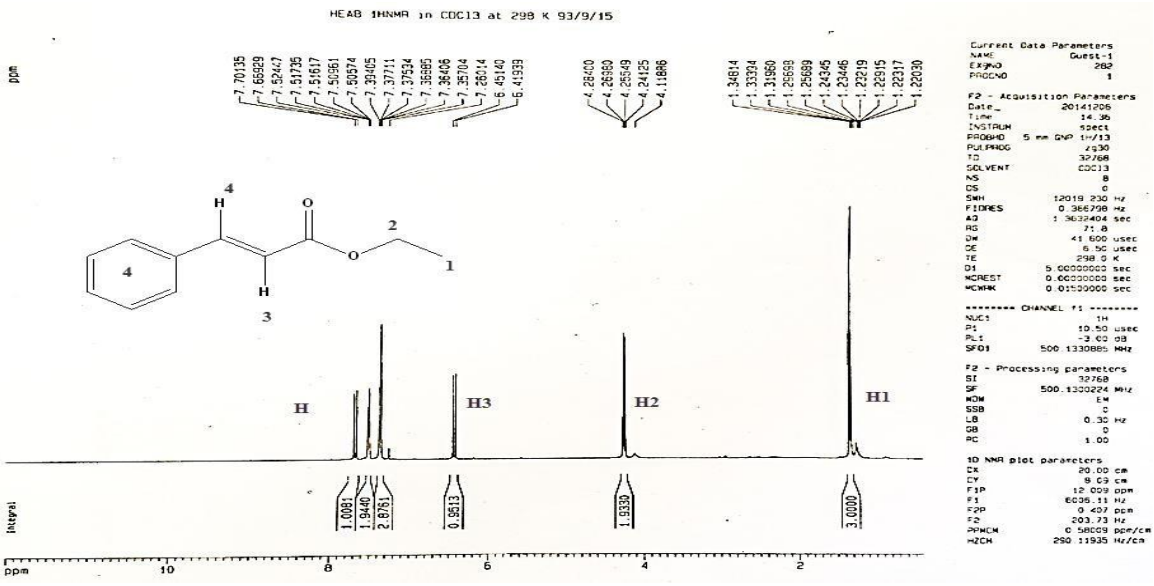

Spectra 36: ^{1}H NMR of (8g)

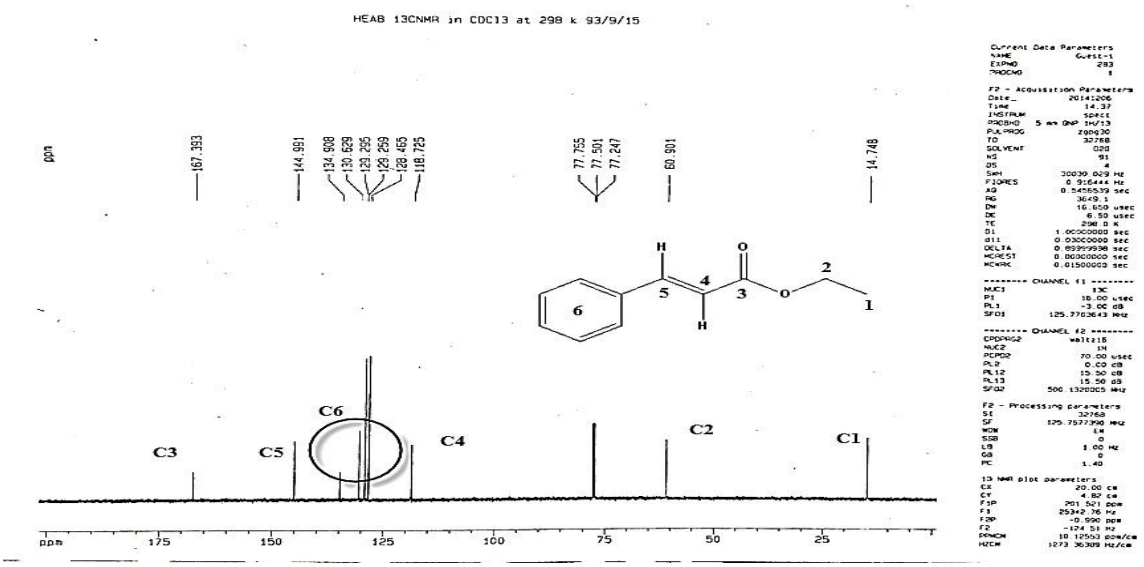

Spectra 37: ^{13}C NMR of (8g)

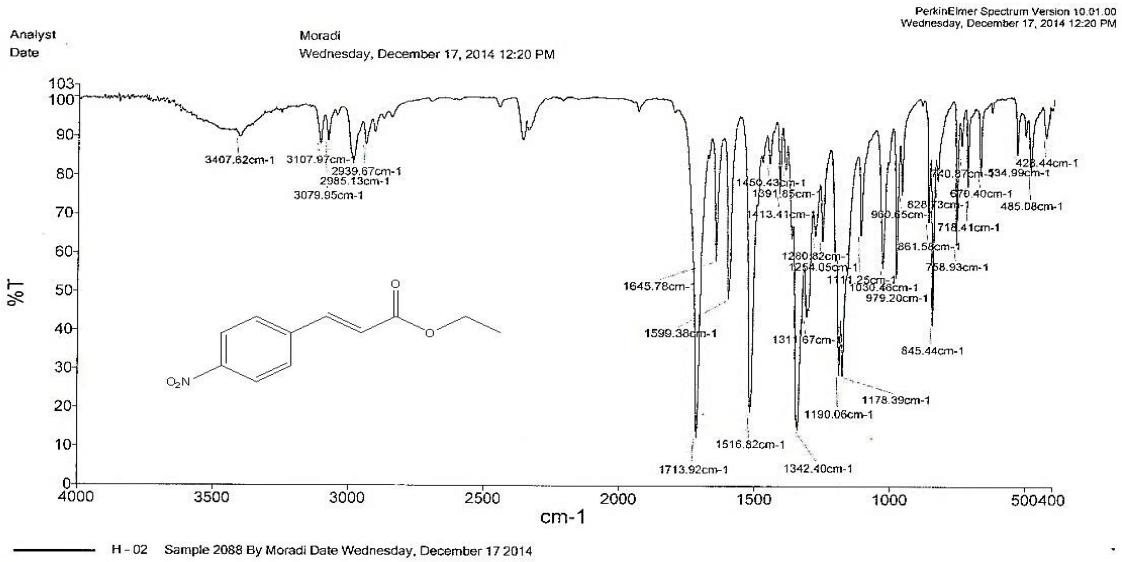

Spectra 38: IR of (9g)

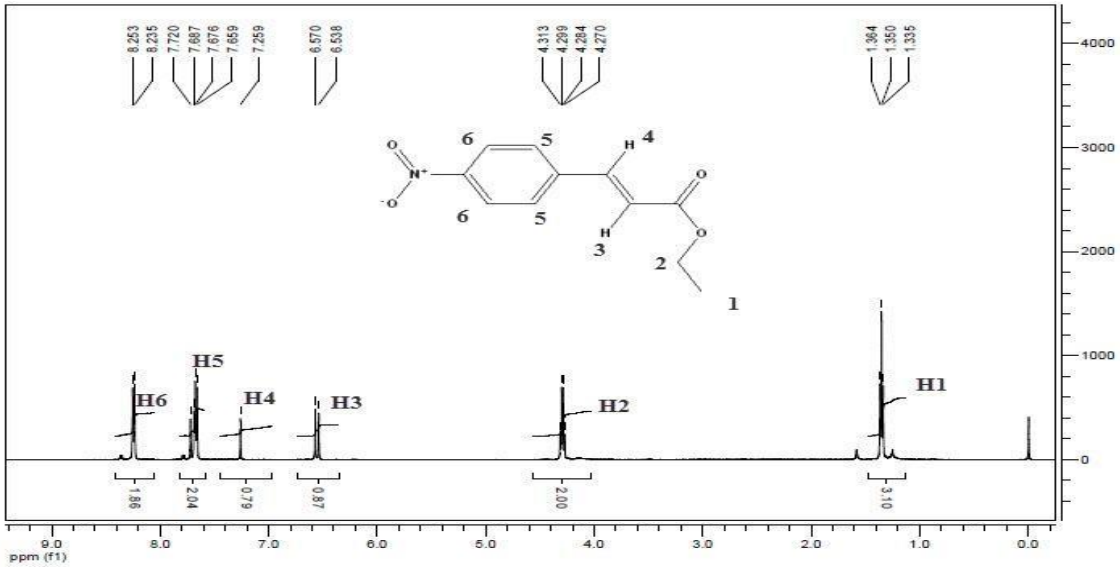

Spectra 39: [1]H NMR of (9g)

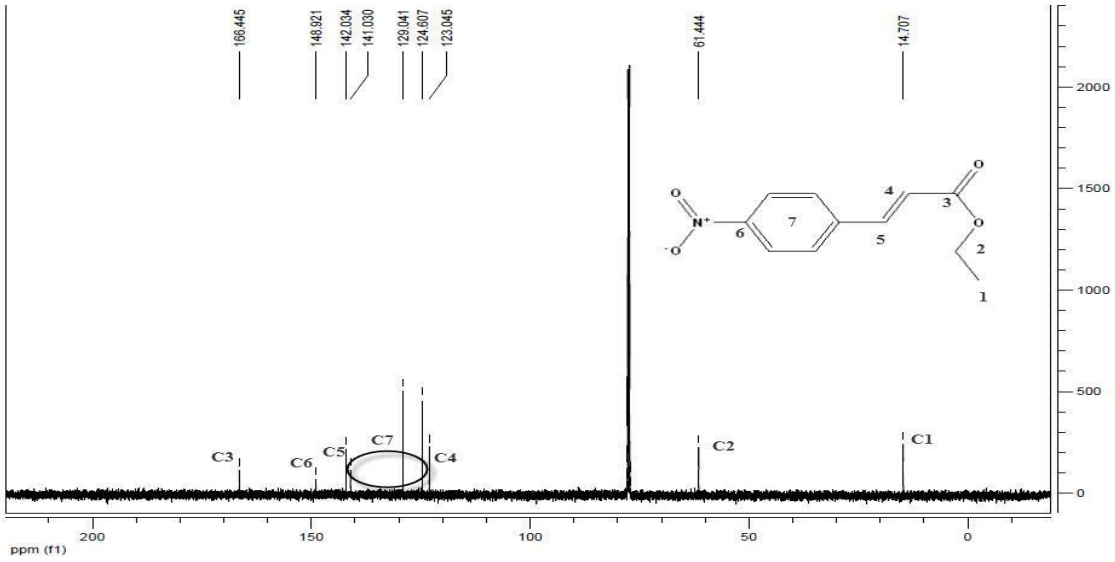

Spectra 40: [13]C NMR of (9g)

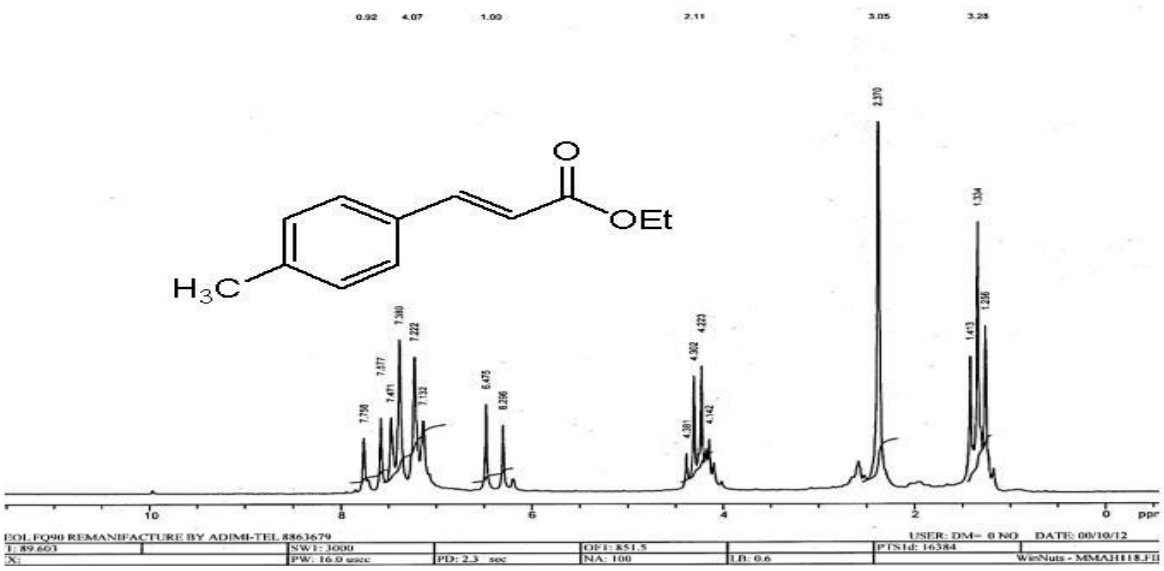

Spectra 41: [1]H NMR of (10g)

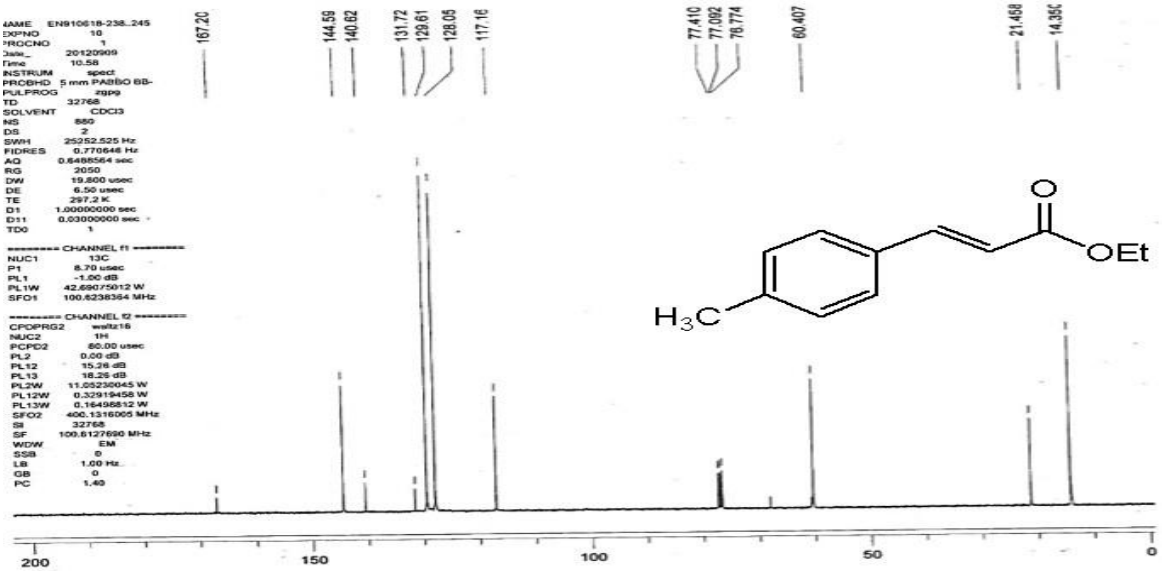

Spectra 42: [13]C NMR of (10g)

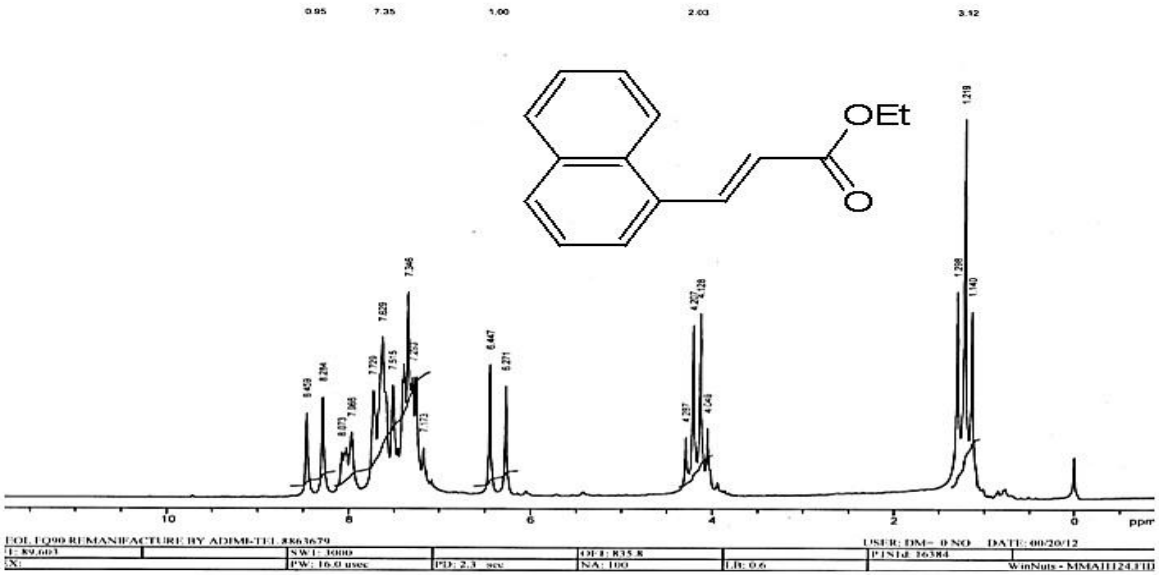

Spectra 43: [1]H NMR of (11g)

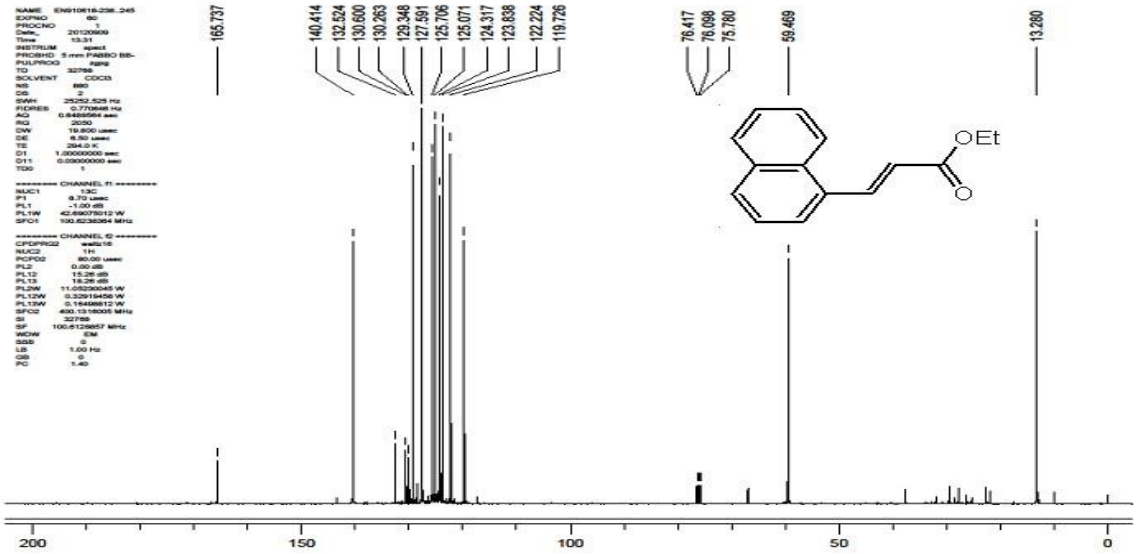

Spectra 44: [13]C NMR of (11g)

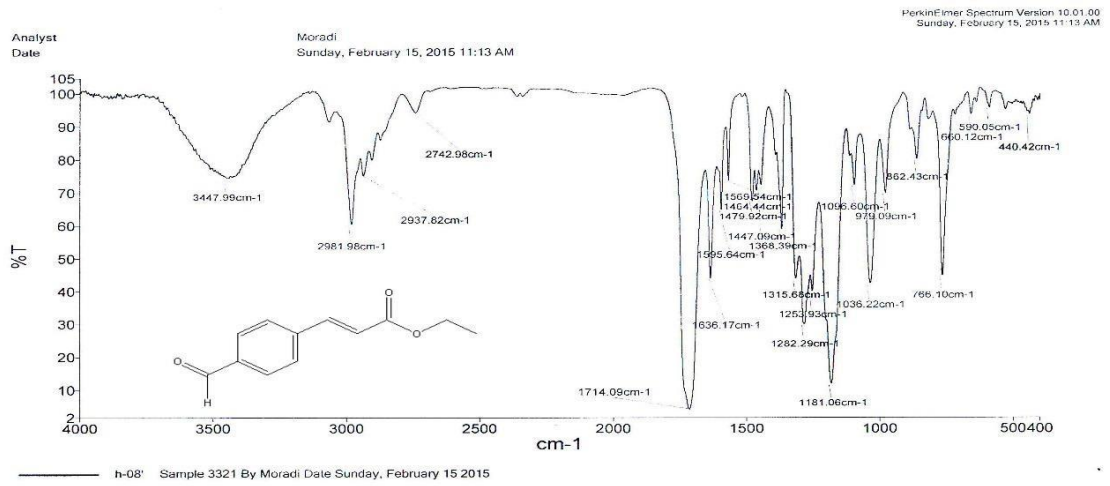

Spectra 45: IR of (12g)

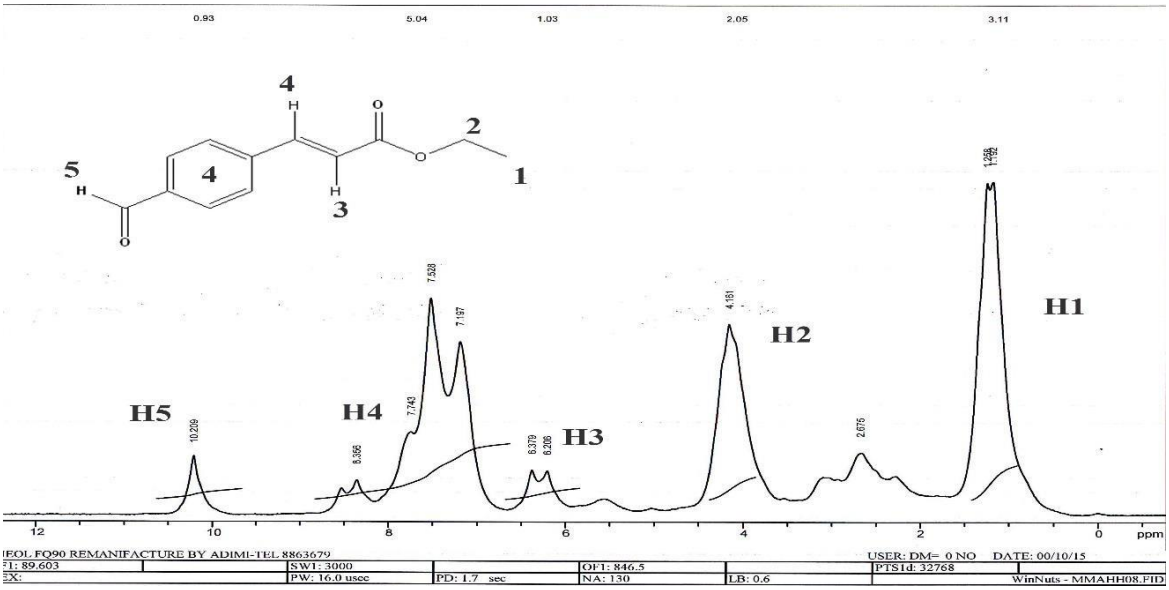

Spectra 46: ^{1}H NMR of (12g)

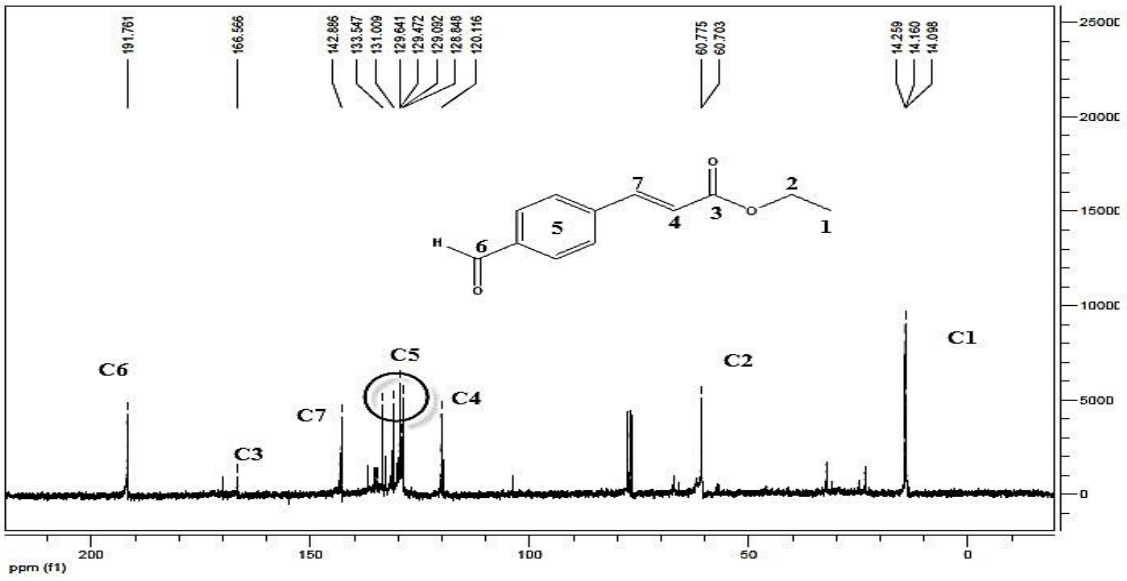

Spectra 47: 13C NMR of (12g)

[1] R. Barik, C. V. Kumar, P. K. Das, M. V. J George, *J. Org. Chem*., 1985, **50**, 4309–4317.
[2] Ö. Aksın, H. TÜrkmen, L. Artok, B. Cetinkaya, C. Ni, O. BÜyÜkgÜngÖr, E. Özkal, *J. Organomet. Chem.*, 2006, **691**, 3027-3036.
[3] H. Hagiwara, Y. Sugawara, K. Isobe, T. Hoshi, T. Suzuki, *Org. Lett*., 2004, **6**, 2325–2328.
[4] E. Shirakawa, H. Otsuka, T. Hayashi, *Chem. Commun*. 2005, **47**, 5885–5886.
[5] J. J. Heynekamp, W. M. Weber, L. A. Hunsaker, A. M. Gonzales, R. A. Orlando, L. M. Deck, D. L. Vander Jagt, *J. Med. Chem*. 2006, **49**, 7182-7189.
[6] C. Xu, J. Gong, S. Yue, Y. Zhu, Y. Wu, *Dalton Trans*., 2006, **39**, (4730-4739.
[7] M. Shibasaki, C. D. J. Boden, A. Kojima, *Tetrahedron*, 1997, **53**, 7371-7395.
[8] P. R. Blakemore, D. K. H. Ho, W. M. Nap, *Org. Biomol. Chem*. 2005, **3**, 1365-1368.
[9] S. Y. Shi, Y. H. Zhang, *Synlett*, 2007, **12**,1843-1850.
[10] S. Gibson, D. F. Foster, G. R. Eastham, R. P. Tooze, D. J. Cole-Hamilton, *Chem. Commun*., 2001, **8**, 779-780.